Towards *ab initio* simulation of quantum plasmas and warm dense matter

Michael Bonitz, Simon Groth, Tobias Dornheim†, Jan Vorberger*, Kushal Ramakrishna*, Zhandos Moldabekov**, Alexey Filinov, and Shen Zhang,

in collaboration with Travis Sjostrom[1], Fionn D. Malone[2], W.M.C. Foulkes[3], and Frank Graziani[2]

Institute of Theoretical Physics and Astrophysics, Kiel University
† Center for Advanced Systems Understanding, * Helmholtz-Zentrum Dresden
** Al Farabi University, Almaty, Kazakhstan

[1] Theoretical Division Los Alamos National Laboratory, Los Alamos, New Mexico, USA
[2] Lawrence Livermore National Lab
[3] Department of Physics, Imperial College London, UK

November 2019
www.theo-physik.uni-kiel.de/bonitz

Kiel: sailing capital

Kiel: capital of Schleswig-Holstein, sailing and science city

Kiel: capital of Schleswig-Holstein, sailing and science city

- **Place of birth and first professorship of Max Planck**

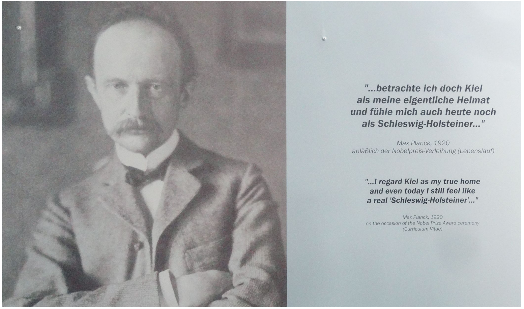

Kiel: capital of Schleswig-Holstein, sailing and science city

- **Place of birth and first professorship of Max Planck**

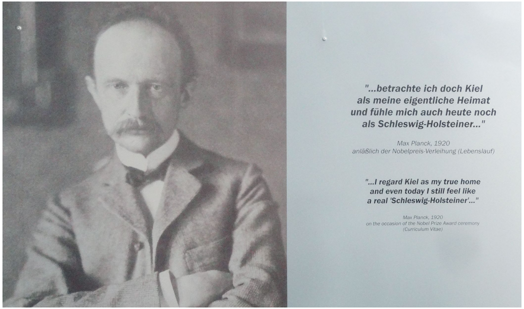

- **114 years later: Chair Statistical Physics:**
  - Classical and quantum plasmas
  - strongly correlated solids

  - Quantum kinetic theory, nonequilbirium Green functions
  - *Ab initio* simulations (MD, quantum Monte Carlo, DFT)
  - Quantum hydrodynamics

Warm Dense Matter: Occurences and Applications

- **Astrophysics:**
  - Giant planet interiors (e.g. Jupiter)
  - Brown dwarfs
  - Meteor Impacts

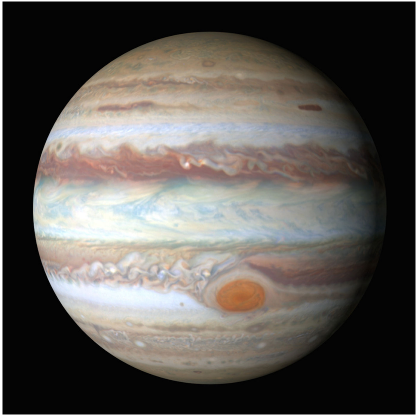

Source: Sci-News.com [Img4]

Warm Dense Matter: Occurences and Applications

- **Astrophysics:**
  - Giant planet interiors (e.g. Jupiter)
  - Brown dwarfs
  - Meteor Impacts
- **Experiments:**
  - Inertial confinement fusion

    Potential abundance of clean energy!

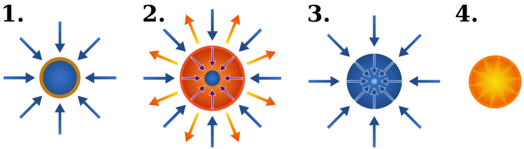

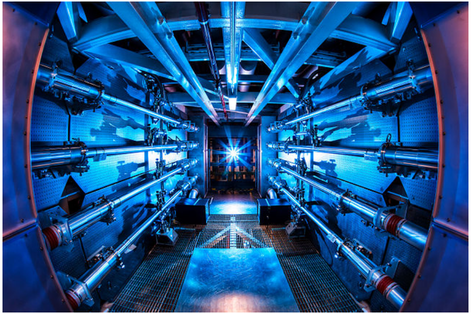

Source: en.wikipedia.org [Img5] and arstechnica.com [Img6]

Warm Dense Matter: Occurences and Applications

- **Astrophysics:**
  - Giant planet interiors (e.g. Jupiter)
  - Brown dwarfs
  - Meteor Impacts
- **Experiments:**
  - Inertial confinement fusion

    Potential abundance of clean energy!

WDM conditions routinely realized at large research facilities
$\rightarrow$ Equation of state, $S(\mathbf{q},\omega)$, etc.

National Ignition Facility (Livermore, California)

area: $70000m^2$
cost: $\sim$1 billion Dollar
Source: C. Stolz, *Phil. Trans. R. Soc. A* **370**, 4115 (2012) [Img7]

Warm Dense Matter and quantum plasmas: relevant parameters

- **Extreme and exotic state of matter:**
  $\rightarrow$ High temperature: $T \sim 10^4 - 10^8\ K$
  $\rightarrow$ Solid state density: $n \sim 10^{21} - 10^{27}\ cm^{-3}$

Source: **TD**, S. Groth, and M. Bonitz, *Phys. Reports* **744**, 1-86 (2018)

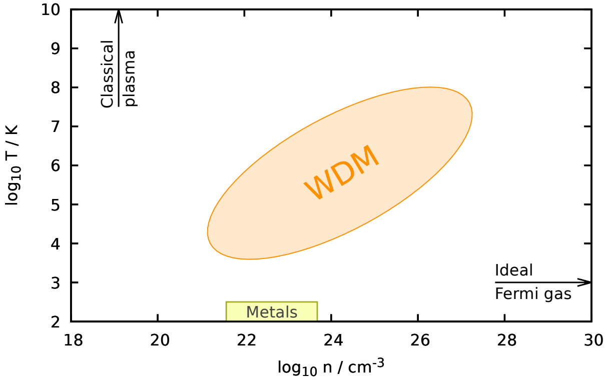

Warm Dense Matter and quantum plasmas: relevant parameters

- **Extreme and exotic state of matter:**
  $\rightarrow$ High temperature: $T \sim 10^4 - 10^8\ K$
  $\rightarrow$ Solid state density: $n \sim 10^{21} - 10^{27}\ cm^{-3}$

- **Characteristic parameters:**

Source: **TD**, S. Groth, and M. Bonitz, *Phys. Reports* **744**, 1-86 (2018)

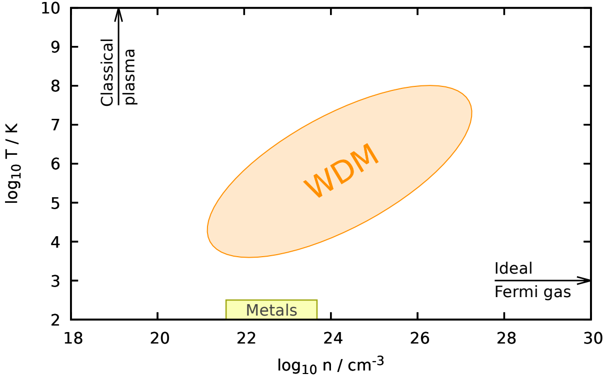

Warm Dense Matter and quantum plasmas: relevant parameters

- **Extreme and exotic state of matter:**
  → High temperature: $T \sim 10^4 - 10^8\ K$
  → Solid state density: $n \sim 10^{21} - 10^{27}\ cm^{-3}$

- **Characteristic parameters:**
  - Density parameter $r_s = \bar{r}/a_B \sim 1$

Source: **TD**, S. Groth, and M. Bonitz, *Phys. Reports* **744**, 1-86 (2018)

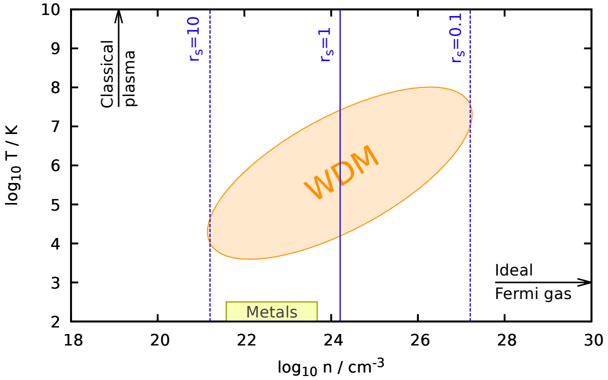

Warm Dense Matter and quantum plasmas: relevant parameters

- **Extreme and exotic state of matter:**

  $\rightarrow$ High temperature: $T \sim 10^4 - 10^8\ K$

  $\rightarrow$ Solid state density: $n \sim 10^{21} - 10^{27}\ cm^{-3}$

- **Characteristic parameters:**
  - Density parameter $r_s = \bar{r}/a_\mathrm{B} \sim 1$
  - Degeneracy temperature $\theta = k_\mathrm{B}T/E_\mathrm{F} \sim 1$

Source: **TD**, S. Groth, and M. Bonitz, *Phys. Reports* **744**, 1-86 (2018)

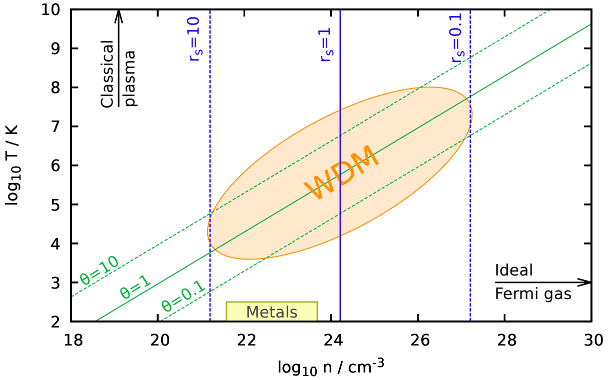

Warm Dense Matter and quantum plasmas: relevant parameters

- **Extreme and exotic state of matter:**

  $\rightarrow$ High temperature: $T \sim 10^4 - 10^8\ K$

  $\rightarrow$ Solid state density: $n \sim 10^{21} - 10^{27}\ cm^{-3}$

- **Characteristic parameters:**
  - Density parameter $r_s = \bar{r}/a_\mathrm{B} \sim 1$
  - Degeneracy temperature $\theta = k_\mathrm{B}T/E_\mathrm{F} \sim 1$
  - $\Theta > 1$: quantum plasma,
    $\Theta < 1$: classical plasma
    Classical coupling parameter $\Gamma = e^2/r_s k_\mathrm{B} T \sim 1$

Source: **TD**, S. Groth, and M. Bonitz, *Phys. Reports* **744**, 1-86 (2018)

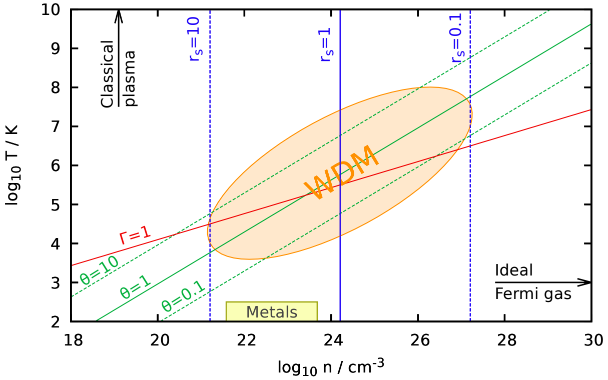

Warm Dense Matter and quantum plasmas: relevant parameters

- **Extreme and exotic state of matter:**

  $\rightarrow$ High temperature: $T \sim 10^4 - 10^8\ K$

  $\rightarrow$ Solid state density: $n \sim 10^{21} - 10^{27}\ cm^{-3}$

- **Characteristic parameters:**
  - Density parameter $r_s = \bar{r}/a_B \sim 1$
  - Degeneracy temperature $\theta = k_B T/E_F \sim 1$
  - $\Theta > 1$: quantum plasma,
    $\Theta < 1$: classical plasma
    Classical coupling parameter $\Gamma = e^2/r_s k_B T \sim 1$

- **Nontrivial interplay of many effects:**
  - Coulomb coupling (non-ideality)

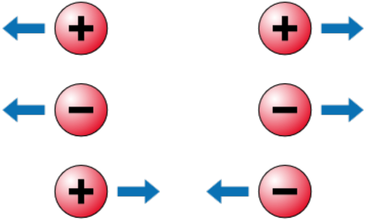

Source: bin-br.at [Img1]

Warm Dense Matter and quantum plasmas: relevant parameters

- **Extreme and exotic state of matter:**
  $\rightarrow$ High temperature: $T \sim 10^4 - 10^8\ K$
  $\rightarrow$ Solid state density: $n \sim 10^{21} - 10^{27}\ cm^{-3}$

- **Characteristic parameters:**
  - Density parameter $r_s = \bar{r}/a_\mathrm{B} \sim 1$
  - Degeneracy temperature $\theta = k_\mathrm{B}T/E_\mathrm{F} \sim 1$
  - $\Theta > 1$: quantum plasma,
    $\Theta < 1$: classical plasma
    Classical coupling parameter $\Gamma = e^2/r_s k_\mathrm{B} T \sim 1$

- **Nontrivial interplay of many effects:**
  - Coulomb coupling (non-ideality)
  - Fermionic exchange (anti-symmetry)

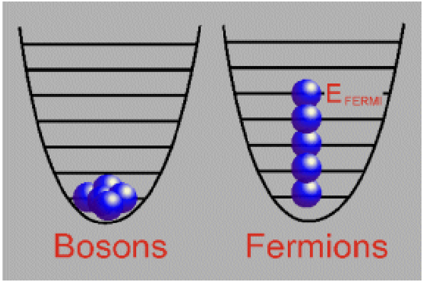

Source: cidehom.com [Img2]

Warm Dense Matter and quantum plasmas: relevant parameters

- **Extreme and exotic state of matter:**

  $\rightarrow$ High temperature: $T \sim 10^4 - 10^8\ K$

  $\rightarrow$ Solid state density: $n \sim 10^{21} - 10^{27}\ cm^{-3}$

- **Characteristic parameters:**
  - Density parameter $r_s = \bar{r}/a_B \sim 1$
  - Degeneracy temperature $\theta = k_B T/E_F \sim 1$
  - $\Theta > 1$: quantum plasma,
    $\Theta < 1$: classical plasma
    Classical coupling parameter $\Gamma = e^2/r_s k_B T \sim 1$

- **Nontrivial interplay of many effects:**
  - Coulomb coupling (non-ideality)
  - Fermionic exchange (anti-symmetry)
  - Thermal excitations (statistical description)

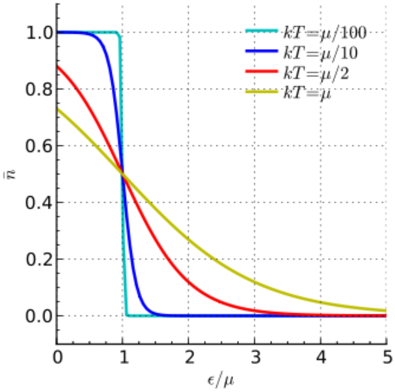

Source: en.wikipedia.org [Img3]

Theoretical problems and simulation methods for WDM

1. WDM in equilibrium

- multiple components free electrons, ions, atoms, and (highly excited) solid
- ⇒ accessible only by DFT+MD

Problems of DFT:

- assumes electrons in ground state
- poor electronic correlations, binding energies, band gaps etc.
- ⇒ accurate static input: QMC

2. WDM out of equilibrium

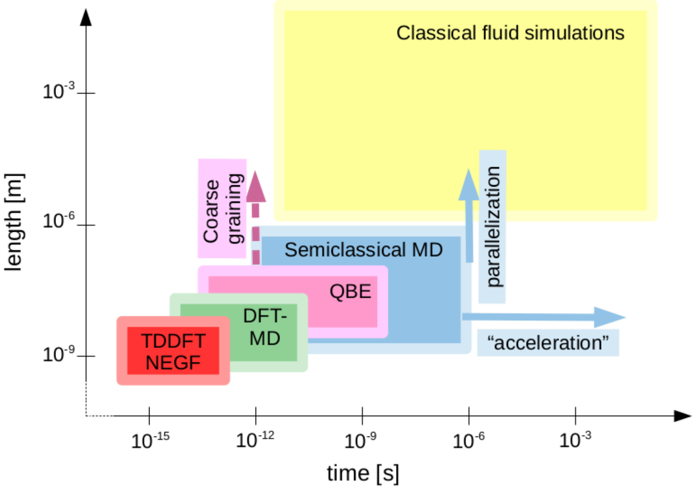

Figure: modified from M. Bonitz *et al.*, *Front. Chem. Science Engin.* (2019)
QBE: quantum Boltzmann equation, NEGF: Nonequilibrium Green functions

Theoretical problems and simulation methods for WDM

1. WDM in equilibrium

- multiple components free electrons, ions, atoms, and (highly excited) solid
- $\Rightarrow$ accessible only by DFT+MD

Problems of DFT:

- assumes electrons in ground state
- poor electronic correlations, binding energies, band gaps etc.
- $\Rightarrow$ accurate static input: QMC

2. WDM out of equilibrium

- fluid simulations (long scales)
- time-dependent DFT (same problems as DFT), quantum kinetic theory, Nonequilibrium Green functions

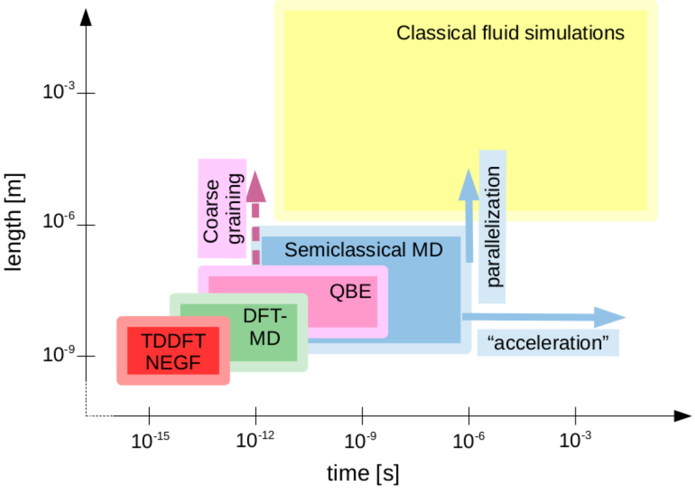

Figure: modified from M. Bonitz *et al.*, *Front. Chem. Science Engin.* (2019)
QBE: quantum Boltzmann equation, NEGF: Nonequilibrium Green functions

Theoretical problems and simulation methods for WDM

1. WDM in equilibrium

- multiple components free electrons, ions, atoms, and (highly excited) solid
- ⇒ accessible only by DFT+MD

Problems of DFT:

- assumes electrons in ground state
- poor electronic correlations, binding energies, band gaps etc.
- ⇒ accurate static input: QMC

2. WDM out of equilibrium

- fluid simulations (long scales)
- time-dependent DFT (same problems as DFT), quantum kinetic theory, Nonequilibrium Green functions
- complementary strengths and limitations need combination of methods

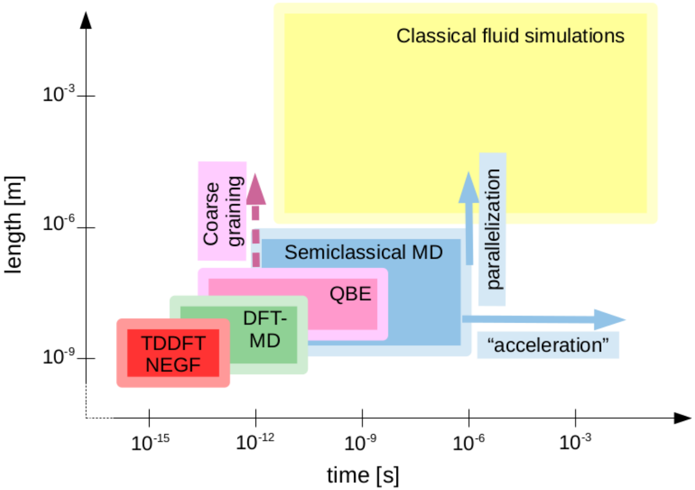

Figure: modified from M. Bonitz *et al.*, *Front. Chem. Science Engin.* (2019)
QBE: quantum Boltzmann equation, NEGF: Nonequilibrium Green functions

Importance of the uniform electron gas (UEG)

Model system of Coulomb interacting quantum electrons in a uniform positive background

Ground state $(T = 0)$:

- Simple model for conduction electrons in metals
- **Exchange-correlation (XC) energy**:

$$e_{xc}(r_s) = e_{tot}(r_s) - e_0(r_s)$$

$\rightarrow$ Input for density functional theory (DFT) simulations (in LDA and GGA)
$\rightarrow$ Parametrization[1] of $e_{xc}(r_s)$ from ground state quantum Monte Carlo data[2]

[1] J.P. Perdew and A. Zunger, PRB **23**, 5048 (1981) [2] D.M. Ceperley and B. Alder, PRL **45**, 566 (1980) [3] N.D. Mermin, Phys. Rev **137**, A1441 (1965)
[4] A.Y. Potekhin and G. Chabrier, *A&A* ***550***, *A43* (2013)

Importance of the uniform electron gas (UEG)

Model system of Coulomb interacting quantum electrons in a uniform positive background

Ground state ($T = 0$):

- Simple model for conduction electrons in metals
- **Exchange-correlation (XC) energy**:

$$e_{xc}(r_s) = e_{tot}(r_s) - e_0(r_s)$$

$\rightarrow$ Input for density functional theory (DFT) simulations (in LDA and GGA)
$\rightarrow$ Parametrization[1] of $e_{xc}(r_s)$ from ground state quantum Monte Carlo data[2]

Warm dense matter ($T \sim T_F$):

- **Thermal DFT**[3]: minimize free energy $F = E - TS$
$\rightarrow$ Requires parametrization of XC **free** energy of UEG:

$$f_{xc}(r_s, \theta) = f_{tot}(r_s, \theta) - f_0(r_s, \theta)$$

- $f_{xc}(r_s, \theta)$ direct input for **EOS models** of astrophysical objects[4]
- $f_{xc}(r_s, \theta)$ contains **complete thermodynamic information** of UEG

---

[1] J.P. Perdew and A. Zunger, PRB **23**, 5048 (1981) [2] D.M. Ceperley and B. Alder, PRL **45**, 566 (1980) [3] N.D. Mermin, Phys. Rev **137**, A1441 (1965)
[4] A.Y. Potekhin and G. Chabrier, *A&A* ***550***, *A43* (2013)

Many parametrizations for f_{xc} based on different approximate approaches:

- Semi-analytical approaches by **Ebeling**[1]
- Dielectric methods, e.g. Singwi-Tosi-Land-Sjölander[2] (**STLS**) and Vashista-Singwi[3] (**VS**)
- Quantum-classical mappings, e.g. Perrot and Dharma-wardana[4] (**PDW**)
- **Most recent:** Fit by Karasiev[5] *et al.* (**KSDT**) to Restricted Path Integral Monte Carlo (**RPIMC**) data[6]

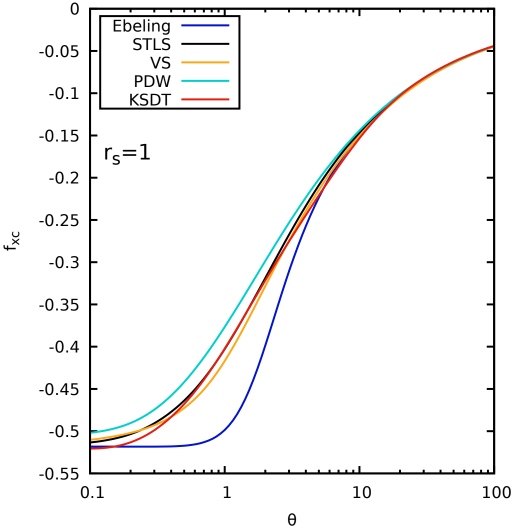

[1] W. Ebeling and H. Lehmann, Ann. Phys. **45**, (1988)
[2] S. Ichimaru, H. Iyetomi, and S. Tanaka, Phys. Rep. **149**, (1987)
[3] T. Sjostrom and J. Dufty, PRB **88**, (2013)
[4] F. Perrot and MWC Dharma-wardana, PRB **62**, (2000)
[5] V.V. Karasiev *et al.*, PRL **112**, (2014)
[6] E.W. Brown *et al.*, PRL **110**, (2013)

Many parametrizations for f_{xc} based on different approximate approaches:

- Semi-analytical approaches by **Ebeling**[1]
- Dielectric methods, e.g. Singwi-Tosi-Land-Sjölander[2] (**STLS**) and Vashista-Singwi[3] (**VS**)
- Quantum-classical mappings, e.g. Perrot and Dharma-wardana[4] (**PDW**)
- **Most recent:** Fit by Karasiev[5] *et al.* (**KSDT**) to Restricted Path Integral Monte Carlo (**RPIMC**) data[6]

Accuracy of existing parametrizations for $f_{xc}(r_s, \theta)$ unclear

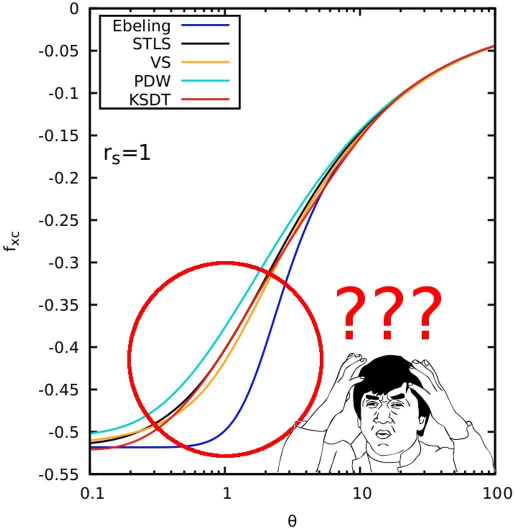

[1] W. Ebeling and H. Lehmann, Ann. Phys. **45**, (1988)
[2] S. Ichimaru, H. Iyetomi, and S. Tanaka, Phys. Rep. **149**, (1987)
[3] T. Sjostrom and J. Dufty, PRB **88**, (2013)
[4] F. Perrot and MWC Dharma-wardana, PRB **62**, (2000)
[5] V.V. Karasiev *et al.*, PRL **112**, (2014)
[6] E.W. Brown *et al.*, PRL **110**, (2013)

Many parametrizations for f_{xc} based on different approximate approaches:

- Semi-analytical approaches by **Ebeling**[1]
- Dielectric methods, e.g. Singwi-Tosi-Land-Sjölander[2] (**STLS**) a
- Quantum Dharma-
- **Most recent:** Fit by Karasiev[5] *et al.* (**KSDT**) to Restricted Path Integral Monte Carlo (**RPIMC**) data[6]

Goal: obtain *ab initio* parametrization of $f_{xc}(r_s, \theta)$

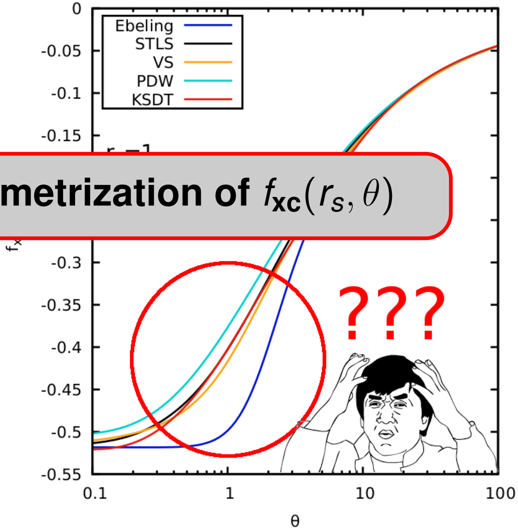

Accuracy of existing parametrizations for $f_{xc}(r_s, \theta)$ unclear

[1] W. Ebeling and H. Lehmann, Ann. Phys. **45**, (1988)
[2] S. Ichimaru, H. Iyetomi, and S. Tanaka, Phys. Rep. **149**, (1987)
[3] T. Sjostrom and J. Dufty, PRB **88**, (2013)
[4] F. Perrot and MWC Dharma-wardana, PRB **62**, (2000)
[5] V.V. Karasiev *et al.*, PRL **112**, (2014)
[6] E.W. Brown *et al.*, PRL **110**, (2013)

Path integral Monte Carlo (PIMC) simulation of the warm dense UEG

- Standard PIMC in warm dense regime severely hampered by ***fermion sign problem***:

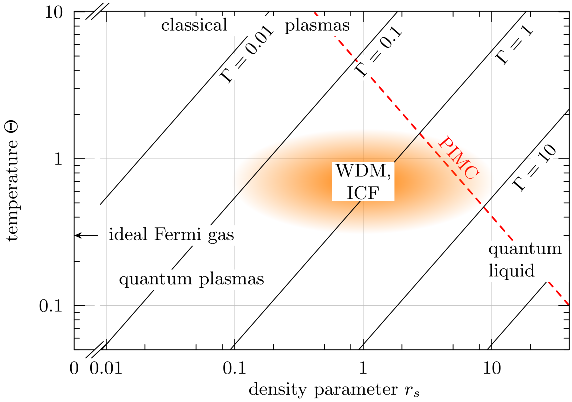

[1] E.W. Brown *et al.*, PRL **110**, 146405 (2013) [2] T. Schoof *et al.*, Phys. Rev. Lett **115**, 130402 (2015) [3] T. Schoof *et al.*, Contrib. Plasma Phys. **51**, 687 (2011)
[4] T. Dornheim *et al.*, New J. Phys. **17**, 073017 (2015) [5] T. Dornheim *et al.*, J. Chem. Phys. **143**, 204101 (2015)

Path integral Monte Carlo (PIMC) simulation of the warm dense UEG

- Standard PIMC in warm dense regime severely hampered by ***fermion sign problem***:
  - First results[1] by E. Brown, D. Ceperley *et al.* (2013) based on ***fixed node approximation*** (**RPIMC**)
  - Induces **systematic errors** of unknown magnitude
  - **RPIMC** limited to $r_s \gtrsim 1$

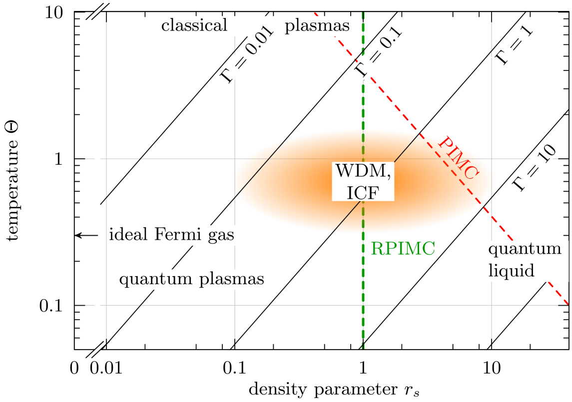

[1] E.W. Brown *et al.*, PRL **110**, 146405 (2013) [2] T. Schoof *et al.*, Phys. Rev. Lett **115**, 130402 (2015) [3] T. Schoof *et al.*, Contrib. Plasma Phys. **51**, 687 (2011)
[4] T. Dornheim *et al.*, New J. Phys. **17**, 073017 (2015) [5] T. Dornheim *et al.*, J. Chem. Phys. **143**, 204101 (2015)

Path integral Monte Carlo (PIMC) simulation of the warm dense UEG

- Standard PIMC in warm dense regime severely hampered by ***fermion sign problem***:
  - First results[1] by E. Brown, D. Ceperley *et al.* (2013) based on ***fixed node approximation*** (**RPIMC**)
  - Induces **systematic errors** of unknown magnitude
  - **RPIMC** limited to $r_s \gtrsim 1$

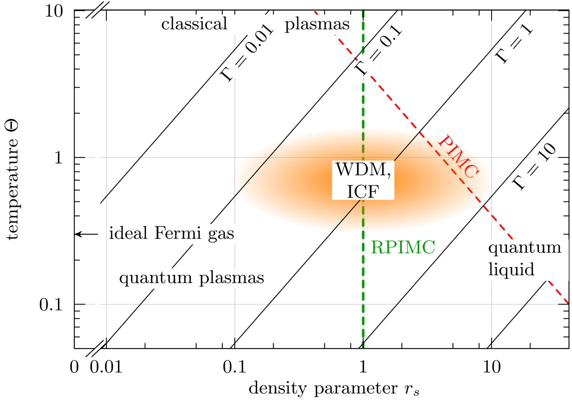

Our approach:

Avoid fermion sign problem by combining two exact and complementary QMC methods:

[1] E.W. Brown *et al.*, PRL **110**, 146405 (2013) [2] T. Schoof *et al.*, Phys. Rev. Lett **115**, 130402 (2015) [3] T. Schoof *et al.*, Contrib. Plasma Phys. **51**, 687 (2011)
[4] T. Dornheim *et al.*, New J. Phys. **17**, 073017 (2015) [5] T. Dornheim *et al.*, J. Chem. Phys. **143**, 204101 (2015)

Path integral Monte Carlo (PIMC) simulation of the warm dense UEG

- Standard PIMC in warm dense regime severely hampered by ***fermion sign problem***:
  - First results[1] by E. Brown, D. Ceperley *et al.* (2013) based on ***fixed node approximation*** (**RPIMC**)
  - Induces **systematic errors** of unknown magnitude
  - **RPIMC** limited to $r_s \gtrsim 1$

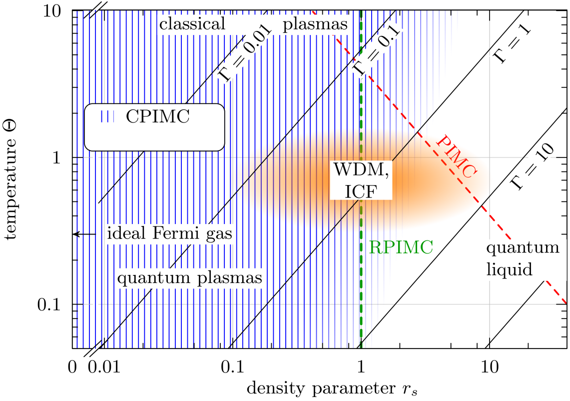

Our approach:

Avoid fermion sign problem by combining two exact and complementary QMC methods:

1. **Configuration PIMC (CPIMC)**[2,3]

$\rightarrow$ Excels at high density $r_s \lesssim 1$ and strong degeneracy

[1] E.W. Brown *et al.*, PRL **110**, 146405 (2013) [2] T. Schoof *et al.*, Phys. Rev. Lett **115**, 130402 (2015) [3] T. Schoof *et al.*, Contrib. Plasma Phys. **51**, 687 (2011)
[4] T. Dornheim *et al.*, New J. Phys. **17**, 073017 (2015) [5] T. Dornheim *et al.*, J. Chem. Phys. **143**, 204101 (2015)

Path integral Monte Carlo (PIMC) simulation of the warm dense UEG

- Standard PIMC in warm dense regime severely hampered by ***fermion sign problem***:
  - First results[1] by E. Brown, D. Ceperley *et al.* (2013) based on ***fixed node approximation*** (**RPIMC**)
  - Induces **systematic errors** of unknown magnitude
  - **RPIMC** limited to $r_s \gtrsim 1$

Our approach:

Avoid fermion sign problem by combining two exact and complementary QMC methods:

1. **Configuration PIMC (CPIMC)**[2,3]

   $\rightarrow$ Excels at high density $r_s \lesssim 1$ and strong degeneracy

2. **Permutation blocking PIMC (PB-PIMC)**[4,5]

   $\rightarrow$ Extends standard PIMC towards stronger degeneracy

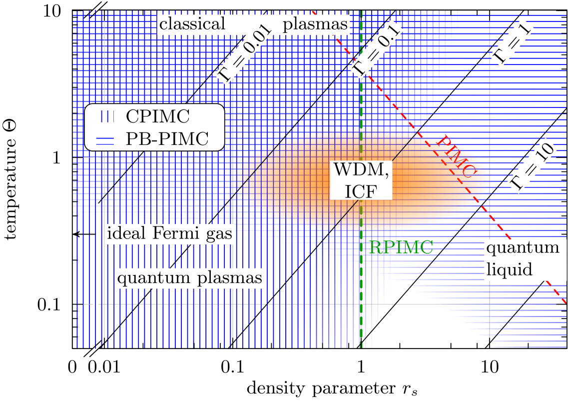

[1] E.W. Brown *et al.*, PRL **110**, 146405 (2013)
[2] T. Schoof *et al.*, Phys. Rev. Lett **115**, 130402 (2015)
[3] T. Schoof *et al.*, Contrib. Plasma Phys. **51**, 687 (2011)
[4] T. Dornheim *et al.*, New J. Phys. **17**, 073017 (2015)
[5] T. Dornheim *et al.*, J. Chem. Phys. **143**, 204101 (2015)

Path integral Monte Carlo (PIMC) simulation of the warm dense UEG

- Standard PIMC in warm dense regime severely hampered by ***fermion sign problem***:
  - First results[1] by E. Brown, D. Ceperley *et al.* (2013) based on ***fixed node approximation*** (**RPIMC**)
  - Induces **systematic errors** of unknown magnitude
  - **RPIMC** limited to $r_s \gtrsim 1$

Our approach:

Avoid fermion sign problem by combining two exact and complementary QMC methods:

1. **Configuration PIMC (CPIMC)**[2,3]

   → Excels at high density $r_s \lesssim 1$ and strong degeneracy
2. **Permutation blocking PIMC (PB-PIMC)**[4,5]

   → Extends standard PIMC towards stronger degeneracy

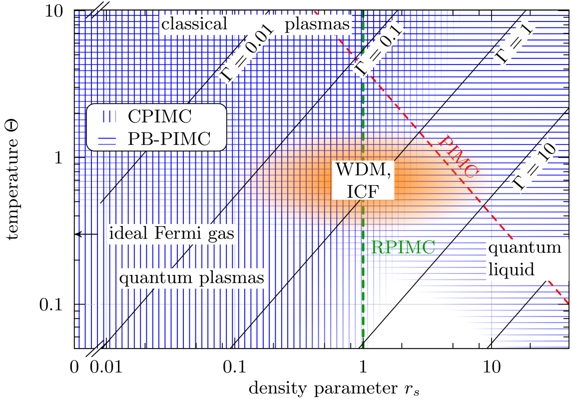

***Ab initio* simulations over broad range of parameters**

[1] E.W. Brown *et al.*, PRL **110**, 146405 (2013) [2] T. Schoof *et al.*, Phys. Rev. Lett **115**, 130402 (2015) [3] T. Schoof *et al.*, Contrib. Plasma Phys. **51**, 687 (2011)
[4] T. Dornheim *et al.*, New J. Phys. **17**, 073017 (2015) [5] T. Dornheim *et al.*, J. Chem. Phys. **143**, 204101 (2015)

Exact exchange-correlation energy $E_{xc} = E - E_0$ (E_0: ideal energy)
($N = 33$ spin-polarized electrons, $\theta \geq 0.5$, $\forall\ r_s$)

- **RPIMC** limited to $r_s \geq 1$

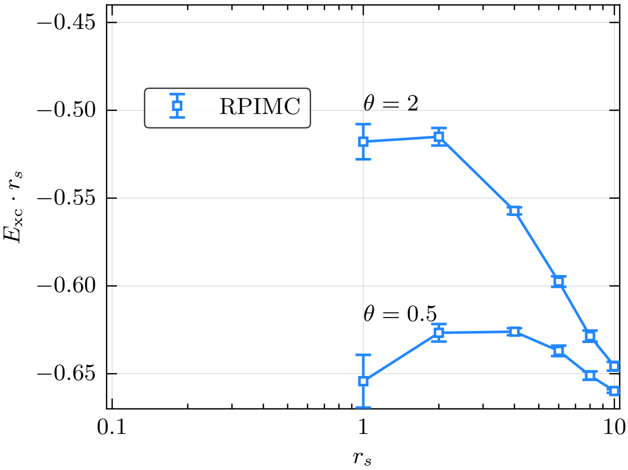

[1] S. Groth *et al.*, Phys. Rev. B **93**, 085102 (2016) [2] T. Dornheim *et al.*, Phys. Rev. B **93**, 205134 (2016)
[3] F.D. Malone *et al.*, Phys. Rev. Lett. **117**, 115701 (2016) [4] T. Schoof *et al.*, Phys. Rev. Lett. (2015)

Exact exchange-correlation energy $E_{xc} = E - E_0$ (E_0: ideal energy) ($N = 33$ spin-polarized electrons, $\theta \geq 0.5$, $\forall\, r_s$)

- **RPIMC** limited to $r_s \geq 1$
- **CPIMC** excels at high density

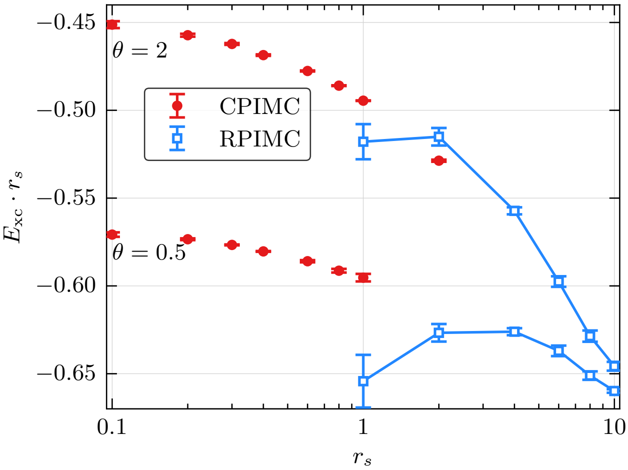

[1] S. Groth *et al.*, Phys. Rev. B **93**, 085102 (2016)
[2] T. Dornheim *et al.*, Phys. Rev. B **93**, 205134 (2016)
[3] F.D. Malone *et al.*, Phys. Rev. Lett. **117**, 115701 (2016)
[4] T. Schoof *et al.*, Phys. Rev. Lett. (2015)

Exact exchange-correlation energy $E_{xc} = E - E_0$ (E_0: ideal energy) ($N = 33$ spin-polarized electrons, $\theta \geq 0.5$, $\forall\ r_s$)

- **RPIMC** limited to $r_s \geq 1$
- **CPIMC** excels at high density
- **PB-PIMC** applicable at $\theta \gtrsim 0.5$

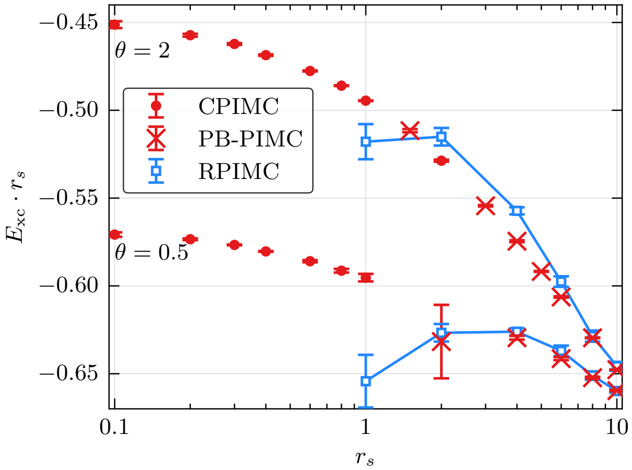

[1] S. Groth *et al.*, Phys. Rev. B **93**, 085102 (2016) [2] T. Dornheim *et al.*, Phys. Rev. B **93**, 205134 (2016)
[3] F.D. Malone *et al.*, Phys. Rev. Lett. **117**, 115701 (2016) [4] T. Schoof *et al.*, Phys. Rev. Lett. (2015)

Exact exchange-correlation energy $E_{xc} = E - E_0$ (E_0: ideal energy) ($N = 33$ spin-polarized electrons, $\theta \geq 0.5$, $\forall\ r_s$)

- **RPIMC** limited to $r_s \geq 1$
- **CPIMC** excels at high density
- **PB-PIMC** applicable at $\theta \gtrsim 0.5$

Combination[1] yields exact results over entire density range down to $\theta \sim 0.5$

- Also applies to the **unpolarized** UEG[2]
- confirmed by independent **DMQMC** simulations[3]

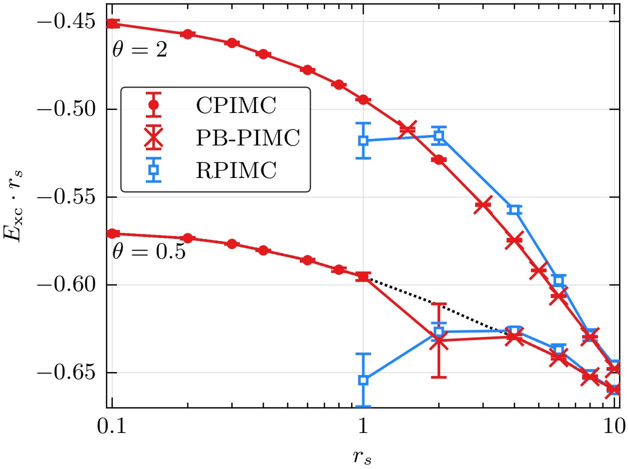

[1] S. Groth *et al.*, Phys. Rev. B **93**, 085102 (2016)
[2] T. Dornheim *et al.*, Phys. Rev. B **93**, 205134 (2016)
[3] F.D. Malone *et al.*, Phys. Rev. Lett. **117**, 115701 (2016)
[4] T. Schoof *et al.*, Phys. Rev. Lett. (2015)

The first complete *ab initio*-based thermodynamic data for the UEG at WDM conditions: $0 \leq r_s \leq 20$, $0 \leq \Theta \leq 10$, $0 \leq \xi \leq 1$, error below 0.3%

1. Accurate results for $f_{\rm xc}$ for finite N for paramagnetic and ferromagnetic cases[1,2]

---

[1] T. Schoof *et al.*, PRL **115**, 130402 (2015) [2] S. Groth *et al.*, PRB **93**, 085102 (2016) [5] T. Dornheim *et al.*, Phys. Plasmas **24**, 056303 (2017)
[3] T. Dornheim *et al.*, PRL **117**, 156403 (2016) [4] S. Groth *et al.*, PRL **119**, 135001 (2017) [6] T. Dornheim, S. Groth, and M. Bonitz, *Physics Reports* **744**, 1-86 (2018)
[7] V. Karasiev *et al.*, Phys. Rev. B (2019): in part incorrect statements; [8] T. Dornheim *et al.*, Phys. Rev. Lett. (2018)

The first complete *ab initio*-based thermodynamic data for the UEG at WDM conditions: $0 \le r_s \le 20, \quad 0 \le \Theta \le 10, \quad 0 \le \xi \le 1$, error below 0.3%

1. Accurate results for f_{xc} for finite N for paramagnetic and ferromagnetic cases[1,2]
2. Accurate finite size corrections and extrapolation to thermodynamic limit[3], $N \to \infty$
3. Connect our data to ground state data, cover entire temperature range[4]

---

[1] T. Schoof *et al.*, PRL **115**, 130402 (2015) [2] S. Groth *et al.*, PRB **93**, 085102 (2016) [5] T. Dornheim *et al.*, Phys. Plasmas **24**, 056303 (2017)
[3] T. Dornheim *et al.*, PRL **117**, 156403 (2016) [4] S. Groth *et al.*, PRL **119**, 135001 (2017) [6] T. Dornheim, S. Groth, and M. Bonitz, *Physics Reports* **744**, 1-86 (2018)
[7] V. Karasiev *et al.*, Phys. Rev. B (2019): in part incorrect statements; [8] T. Dornheim *et al.*, Phys. Rev. Lett. (2018)

The first complete *ab initio*-based thermodynamic data for the UEG at WDM conditions: $0 \le r_s \le 20, \quad 0 \le \Theta \le 10, \quad 0 \le \xi \le 1$, error below 0.3%

1. Accurate results for $f_{\rm xc}$ for finite N for paramagnetic and ferromagnetic cases[1,2]
2. Accurate finite size corrections and extrapolation to thermodynamic limit[3], $N \to \infty$
3. Connect our data to ground state data, cover entire temperature range[4]
4. New data for intermediate spin polarizations[4,6], 3-dimensional analytical parametrization[7], $f_{\rm xc}(r_s, \Theta, \xi)$
   $f_{\rm xc}$-functional implemented in Libxc (LDA_XC_GDSMFB)

Comments and outlook:

- first unbiased tests of many earlier models and fits[5,6]: STLS, VS, Ichimaru, Dharma wardana, Ebeling, Green functions (Kraeft, Vorberger, Rehr...) etc.: benchmark data allow for model improvement
- earlier fit (KSDT) by Karasiev *et al.*: tested and subsequently corrected, *now good agreement* with GDSMFB

---

[1] T. Schoof *et al.*, PRL **115**, 130402 (2015) [2] S. Groth *et al.*, PRB **93**, 085102 (2016) [5] T. Dornheim *et al.*, Phys. Plasmas **24**, 056303 (2017)
[3] T. Dornheim *et al.*, PRL **117**, 156403 (2016) [4] S. Groth *et al.*, PRL **119**, 135001 (2017) [6] T. Dornheim, S. Groth, and M. Bonitz, *Physics Reports* **744**, 1-86 (2018)
[7] V. Karasiev *et al.*, Phys. Rev. B (2019): in part incorrect statements; [8] T. Dornheim *et al.*, Phys. Rev. Lett. (2018)

The first complete *ab initio*-based thermodynamic data for the UEG at WDM conditions: $0 \leq r_s \leq 20, \quad 0 \leq \Theta \leq 10, \quad 0 \leq \xi \leq 1$, error below 0.3%

1. Accurate results for $f_{\rm xc}$ for finite N for paramagnetic and ferromagnetic cases[1,2]
2. Accurate finite size corrections and extrapolation to thermodynamic limit[3], $N \to \infty$
3. Connect our data to ground state data, cover entire temperature range[4]
4. New data for intermediate spin polarizations[4,6], 3-dimensional analytical parametrization[7], $f_{\rm xc}(r_s, \Theta, \xi)$
   $f_{\rm xc}$-functional implemented in Libxc (LDA_XC_GDSMFB)

Comments and outlook:

- first unbiased tests of many earlier models and fits[5,6]: STLS, VS, Ichimaru, Dharma wardana, Ebeling, Green functions (Kraeft, Vorberger, Rehr...) etc.: benchmark data allow for model improvement
- earlier fit (KSDT) by Karasiev *et al.*: tested and subsequently corrected, *now good agreement* with GDSMFB
- derivatives $\partial f_{\rm xc}/\partial n$ and $\partial f_{\rm xc}/\partial T$ potentially inaccurate; $\Rightarrow$ *fits to separate ab initio data needed*

---

[1] T. Schoof *et al.*, PRL **115**, 130402 (2015) [2] S. Groth *et al.*, PRB **93**, 085102 (2016) [5] T. Dornheim *et al.*, Phys. Plasmas **24**, 056303 (2017)
[3] T. Dornheim *et al.*, PRL **117**, 156403 (2016) [4] S. Groth *et al.*, PRL **119**, 135001 (2017) [6] T. Dornheim, S. Groth, and M. Bonitz, *Physics Reports* **744**, 1-86 (2018)
[7] V. Karasiev *et al.*, Phys. Rev. B (2019): in part incorrect statements; [8] T. Dornheim *et al.*, Phys. Rev. Lett. (2018)

Benchmarks for existing and future models and fits:

S. Groth *et al.*, *PRL* (2017)

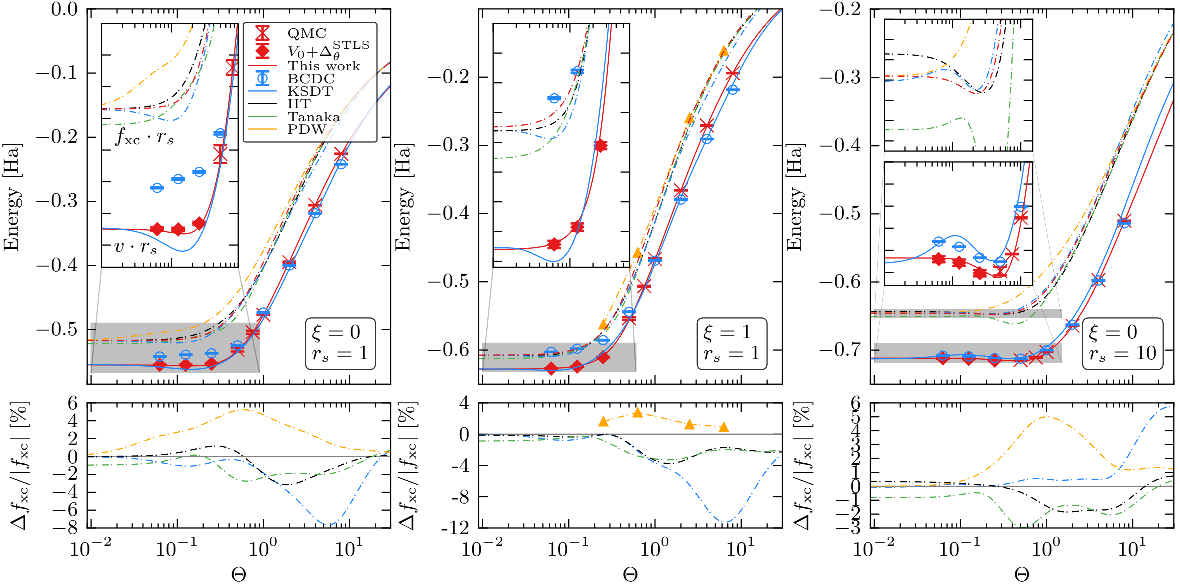

Benchmarks for existing and future models and fits:

S. Groth *et al.*, *PRL* (2017)

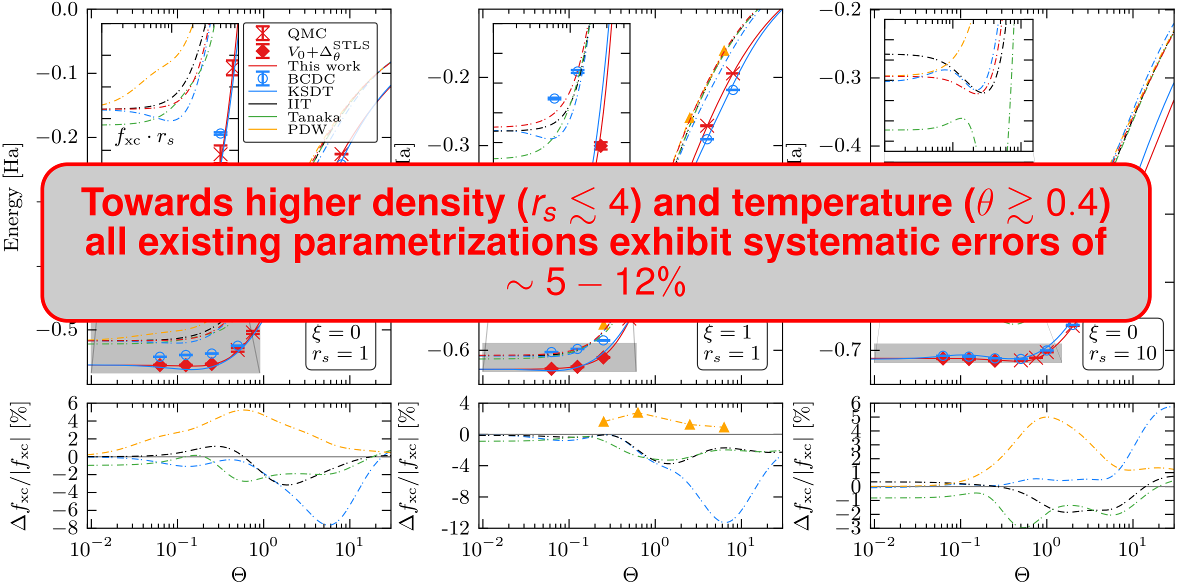

Towards higher density ($r_s \lesssim 4$) and temperature ($\theta \gtrsim 0.4$) all existing parametrizations exhibit systematic errors of $\sim 5 - 12\%$

Impact of finite-T functional on DFT-MD simulations: dense hydrogen[1]

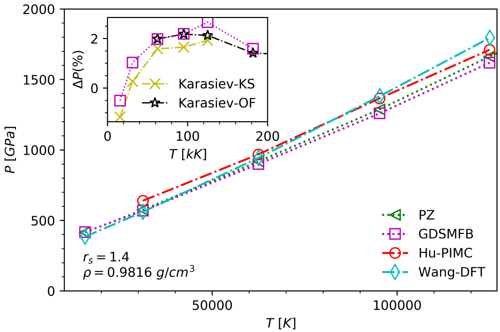

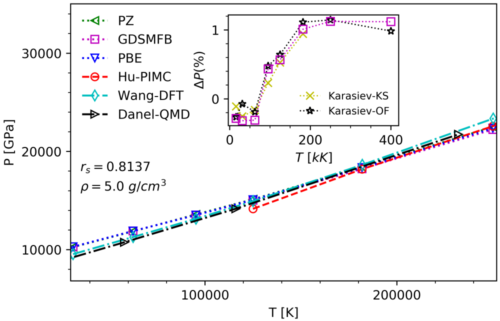

GDSMFB: present finite-T functional, **PZ**: Perdew, Zunger (1981), **PBE**: Perdew, Burke, Enzerhof (1996)
Hu-PIMC: Hu, Militzer, PRB 2011; **Wang-DFT**: Orbital-free MD, Phys. Plasmas (2013)
Karasiev *et al.*, PRE (2016)

[1] Kushal Ramakrishna, unpublished

Impact of finite-T functional: dense hydrogen, electronic pressure[2]

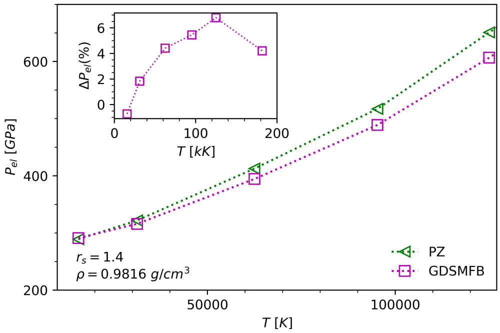

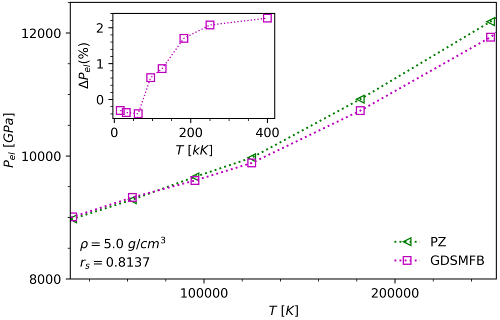

significantly larger differences in specific heat, susceptibilities

[2] Kushal Ramakrishna, unpublished

Impact of finite-T functional on DFT-MD simulations: dense carbon[3], $r_s \approx 1.5$

total pressure (left) vs. electronic pressure, $E_F \approx 23\text{eV} \approx 267,000\text{K}$

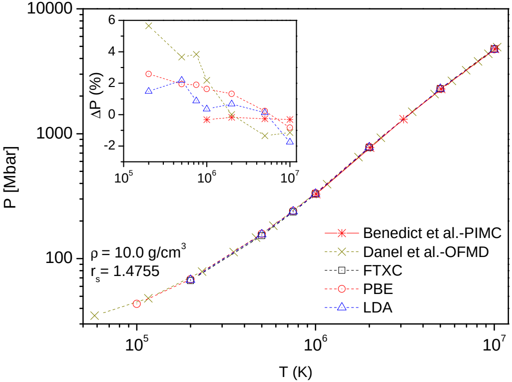

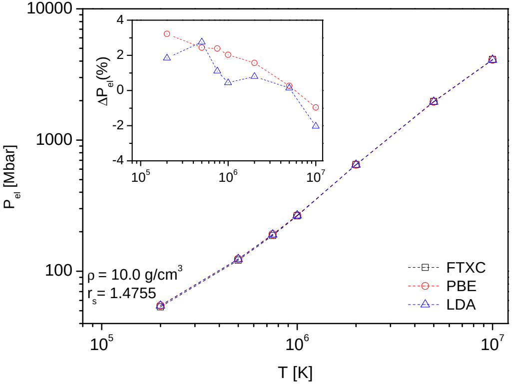

baseline=FTXC: present finite-T functional (GDSMFB), compared to $T = 0$ **PBE** and **LDA**
Danel: Danel, Kazandjian, Piron, PRE 2018;
Benedict: Benedict, Driver, Hamel, Militzer, Qi, Correa, Saul, and Schwegler, Phys. Rev. B (2014)

[3] Shen Zhang, unpublished (highly efficient high-T approach)

Ab initio dynamic (ω-dependent) results for the warm dense UEG

- **Key quantity:** dynamic structure factor

$$S(\mathbf{q},\omega) := \frac{1}{2\pi}\int_{-\infty}^{\infty} \mathrm{d}t\ \underbrace{\langle \hat{n}_{\mathbf{q}}(t)\hat{n}_{-\mathbf{q}}(0)\rangle}_{:=F(\mathbf{q},t)}\ e^{i\omega t}$$

$\rightarrow$ Directly measured in **scattering experiments**

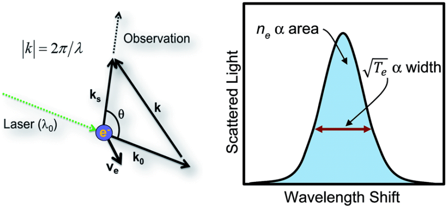

Thomson scattering: signal depends on electron and ion temperature, density and correlations, degree of ionization, band structure of condensed phase etc.

Ab initio dynamic (ω-dependent) results for the warm dense UEG

- **Key quantity:** dynamic structure factor

$$S(\mathbf{q},\omega) := \frac{1}{2\pi}\int_{-\infty}^{\infty} \mathrm{d}t \underbrace{\langle \hat{n}_{\mathbf{q}}(t)\hat{n}_{-\mathbf{q}}(0)\rangle}_{:=F(\mathbf{q},t)} e^{i\omega t}$$

$\rightarrow$ Directly measured in **scattering experiments**

- **Chihara decomposition** applies for non-collective scattering:

$$S(\mathbf{q},\omega) = S_{\text{b-b}}(\mathbf{q},\omega) + S_{\text{b-f}}(\mathbf{q},\omega) + S_{\text{f-f}}(\mathbf{q},\omega)$$

$$\rightarrow S_{\text{f-f}}(\mathbf{q},\omega) \sim S^{\text{UEG}}(\mathbf{q},\omega)$$

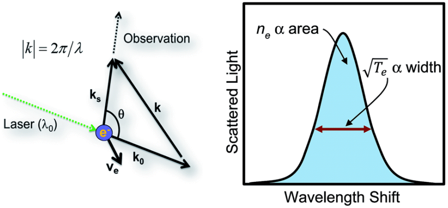

Thomson scattering: signal depends on electron and ion temperature, density and correlations, degree of ionization, band structure of condensed phase etc.

Ab initio dynamic (ω-dependent) results for the warm dense UEG

- **Key quantity:** dynamic structure factor

$$S(\mathbf{q},\omega) := \frac{1}{2\pi}\int_{-\infty}^{\infty} \mathrm{d}t \underbrace{\langle \hat{n}_{\mathbf{q}}(t)\hat{n}_{-\mathbf{q}}(0)\rangle}_{:=F(\mathbf{q},t)} e^{i\omega t}$$

$\rightarrow$ Directly measured in **scattering experiments**

- **Chihara decomposition** applies for non-collective scattering:

$$S(\mathbf{q},\omega) = S_{\text{b-b}}(\mathbf{q},\omega) + S_{\text{b-f}}(\mathbf{q},\omega) + S_{\text{f-f}}(\mathbf{q},\omega)$$

$$\rightarrow S_{\text{f-f}}(\mathbf{q},\omega) \sim S^{\text{UEG}}(\mathbf{q},\omega)$$

- **Practical example:** Fit model for $S(\mathbf{q},\omega;T_e)$ to spectrum to determine electron temperature T_e

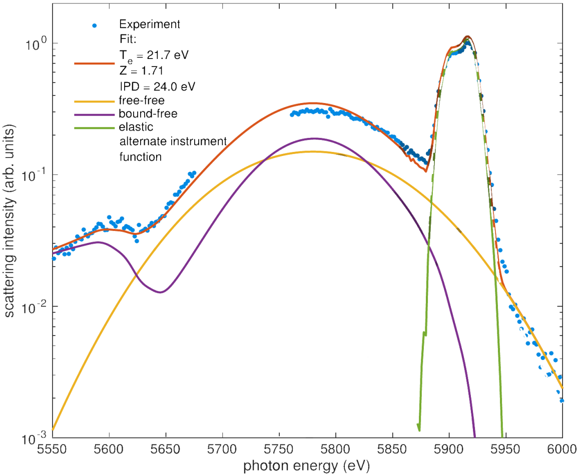

Figure: Scattering spectrum of isochorically heated graphite at LCLS. Taken from D. Kraus *et al.*, *Plasma Phys. Control. Fusion* (2019)

Ab initio dynamic (ω-dependent) results for the warm dense UEG

- **Key quantity:** dynamic structure factor

$$S(\mathbf{q},\omega) := \frac{1}{2\pi}\int_{-\infty}^{\infty} \mathrm{d}t \underbrace{\langle \hat{n}_{\mathbf{q}}(t)\hat{n}_{-\mathbf{q}}(0)\rangle}_{:=F(\mathbf{q},t)} e^{i\omega t}$$

  → Directly measured in **scattering experiments**

- **Chihara decomposition** applies for non-collective scattering:

$$S(\mathbf{q},\omega) = S_{\text{b-b}}(\mathbf{q},\omega) + S_{\text{b-f}}(\mathbf{q},\omega) + S_{\text{f-f}}(\mathbf{q},\omega)$$

$$\rightarrow S_{\text{f-f}}(\mathbf{q},\omega) \sim S^{\text{UEG}}(\mathbf{q},\omega)$$

- **Practical example:** Fit model for $S(\mathbf{q},\omega;T_e)$ to spectrum to determine electron temperature T_e
- **Problem:**
  $F(\mathbf{q},t)$ requires **real time-dependent simulations**

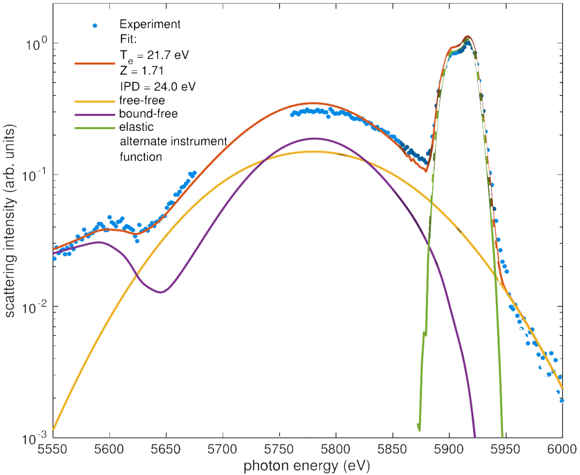

Figure: Scattering spectrum of isochorically heated graphite at LCLS. Taken from D. Kraus *et al.*, *Plasma Phys. Control. Fusion* (2019)

Density correlations: from real time to imaginary time

$$S(\mathbf{q},\omega) := \frac{1}{2\pi}\int_{-\infty}^{\infty} \mathrm{d}t\ \underbrace{\langle \hat{n}_{\mathbf{q}}(t)\hat{n}_{-\mathbf{q}}(0)\rangle}_{:=F(\mathbf{q},t)}\ e^{i\omega t}$$

→ $F(\mathbf{q}, t)$ requires **real time-dependent simulations**
→ Rigorous treatment of correlations **in general not feasible**

[1] Time dependencies denote Heisenberg picture.

Density correlations: from real time to imaginary time

$$S(\mathbf{q},\omega) := \frac{1}{2\pi}\int_{-\infty}^{\infty} \mathrm{d}t\ \underbrace{\langle \hat{n}_{\mathbf{q}}(t)\hat{n}_{-\mathbf{q}}(0)\rangle}_{:=F(\mathbf{q},t)}\ e^{i\omega t}$$

→ $F(\mathbf{q},t)$ requires **real time-dependent simulations**
→ Rigorous treatment of correlations **in general not feasible**

Alternative: analytic continuation $t \to -i\tau$

$$F(\mathbf{q},\tau) = \int_{-\infty}^{\infty} \mathrm{d}\omega\ S(\mathbf{q},\omega)e^{-\tau\omega}\ \forall\ \tau \in [0,\beta]$$

Advantage:
$F(\mathbf{q},\tau)$ accessible within **PIMC** simulations
(**thermodynamic equilibrium** → *ab initio* feasible)

Imaginary-time density-density correlation function:
($\theta = 1$, $r_s = 10$, $N = 34$, $q = 0.63q_F$)

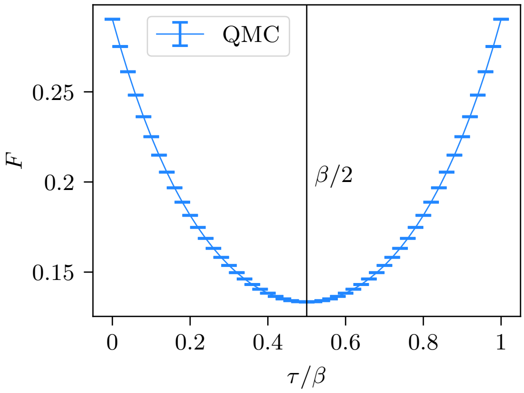

[1] Time dependencies denote Heisenberg picture.

Density correlations: from real time to imaginary time

$$S(\mathbf{q},\omega) := \frac{1}{2\pi}\int_{-\infty}^{\infty} \mathrm{d}t \underbrace{\langle \hat{n}_{\mathbf{q}}(t)\hat{n}_{-\mathbf{q}}(0)\rangle}_{:=F(\mathbf{q},t)} e^{i\omega t}$$

→ $F(\mathbf{q},t)$ requires **real time-dependent simulations**
→ Rigorous treatment of correlations **in general not feasible**

Alternative: analytic continuation $t \rightarrow -i\tau$

$$F(\mathbf{q},\tau) = \int_{-\infty}^{\infty} \mathrm{d}\omega\ S(\mathbf{q},\omega)e^{-\tau\omega}\ \forall\ \tau \in [0,\beta]$$

Advantage:
$F(\mathbf{q},\tau)$ accessible within **PIMC** simulations
(**thermodynamic equilibrium** → *ab initio* feasible)

Disadvantage:
$S(\mathbf{q},\omega)$ requires **inverse Laplace transform**
(**ill-posed problem** → sensitive to statistical errors in F)

Imaginary-time density-density correlation function:
($\theta = 1$, $r_s = 10$, $N = 34$, $q = 0.63q_F$)

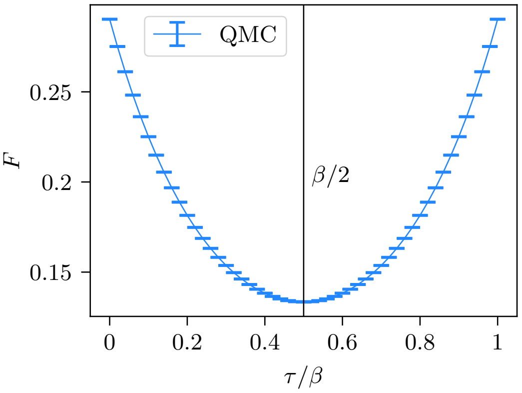

[1] Time dependencies denote Heisenberg picture.

Performing the inverse Laplace transformation for $S(\mathbf{q}, \omega)$

$$F(\mathbf{q}, \tau) = \int_{-\infty}^{\infty} \mathrm{d}\omega \; S(\mathbf{q}, \omega) e^{-\tau\omega} \; \forall \; \tau \in [0, \beta]$$

Known frequency moments: $\langle \omega^{-1} \rangle$, $\langle \omega^{0} \rangle$, $\langle \omega^{1} \rangle$, $\langle \omega^{3} \rangle$

$$\langle \omega^k \rangle \quad = \quad \int_{-\infty}^{\infty} \mathrm{d}\omega \; \omega^k S(\mathbf{q}, \omega)$$

General idea:

- Find / optimize trial spectrum $S^{\mathrm{trial}}(\mathbf{q}, \omega)$ reproducing $F(\mathbf{q}, \tau)$ and frequency moments

[1] E. Vitali *et al.*, *Phys. Rev. B* **82**, 174510 (2010)

Performing the inverse Laplace transformation for $S(\mathbf{q},\omega)$

$$F(\mathbf{q},\tau) = \int_{-\infty}^{\infty} \mathrm{d}\omega\ S(\mathbf{q},\omega) e^{-\tau\omega}\ \forall\ \tau \in [0,\beta]$$

Known frequency moments: $\langle\omega^{-1}\rangle, \langle\omega^{0}\rangle, \langle\omega^{1}\rangle, \langle\omega^{3}\rangle$

$$\langle\omega^k\rangle = \int_{-\infty}^{\infty} \mathrm{d}\omega\ \omega^k S(\mathbf{q},\omega)$$

General idea:

- Find / optimize trial spectrum $S^{\mathrm{trial}}(\mathbf{q},\omega)$ reproducing $F(\mathbf{q},\tau)$ and frequency moments

Method 1: Genetic Inversion via Falsification of Theories[1] (GIFT)

- Stochastically evolve set of trial spectra $\{S_i^{\mathrm{trial}}(\mathbf{q},\omega)\}$

Dynamic structure factor of the UEG:
$(\theta = 1, r_s = 10, N = 34, k = 0.63k_F)$

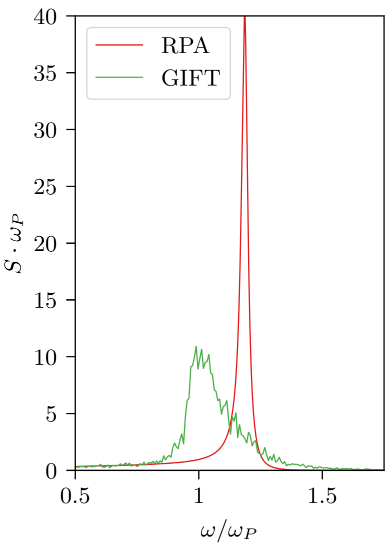

[1] E. Vitali *et al.*, *Phys. Rev. B* **82**, 174510 (2010)

Performing the inverse Laplace transformation for $S(\mathbf{q},\omega)$

$$F(\mathbf{q},\tau) = \int_{-\infty}^{\infty} \mathrm{d}\omega \ S(\mathbf{q},\omega) e^{-\tau\omega} \ \forall \ \tau \in [0,\beta]$$

Known frequency moments: $\langle\omega^{-1}\rangle, \langle\omega^{0}\rangle, \langle\omega^{1}\rangle, \langle\omega^{3}\rangle$

$$\langle\omega^k\rangle = \int_{-\infty}^{\infty} \mathrm{d}\omega \ \omega^k S(\mathbf{q},\omega)$$

General idea:

- Find / optimize trial spectrum $S^{\mathrm{trial}}(\mathbf{q},\omega)$ reproducing $F(\mathbf{q},\tau)$ and frequency moments

Method 1: Genetic Inversion via Falsification of Theories[1] (GIFT)

- Stochastically evolve set of trial spectra $\{S_i^{\mathrm{trial}}(\mathbf{q},\omega)\}$

Method 2: Machine learning (ML)

- Compute versatile test set $\{F_i, S_i\}$, $i = 1, \ldots, 10^6$
- Train **neural net** to perform mapping $\{F, \langle\omega^{-1}\rangle \ldots \langle\omega^3\rangle\} \to S$

Dynamic structure factor of the UEG:
$(\theta = 1, r_s = 10, N = 34, k = 0.63 k_F)$

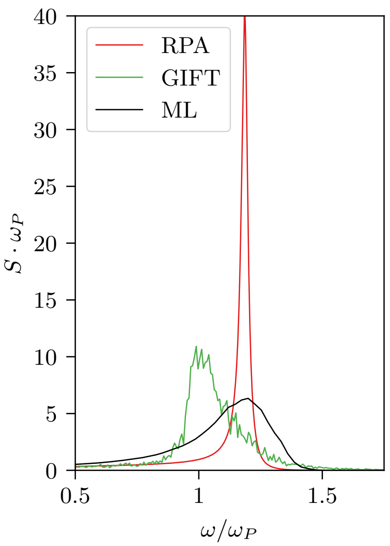

[1] E. Vitali *et al.*, *Phys. Rev. B* **82**, 174510 (2010)

Performing the inverse Laplace transformation for $S(\mathbf{q},\omega)$

$$F(\mathbf{q},\tau) = \int_{-\infty}^{\infty} \mathrm{d}\omega \ S(\mathbf{q},\omega) e^{-\tau\omega} \ \forall \ \tau \in [0,\beta]$$

Known frequency moments: $\langle \omega^{-1} \rangle$, $\langle \omega^{0} \rangle$, $\langle \omega^{1} \rangle$, $\langle \omega^{3} \rangle$

$$\langle \omega^k \rangle = \int_{-\infty}^{\infty} \mathrm{d}\omega \ \omega^k S(\mathbf{q},\omega)$$

GIFT and ML spectra reproduce correct F and $\langle \omega^{-1} \rangle - \langle \omega^{3} \rangle$

$\rightarrow$ Knowledge of F and $\langle \omega^{-1} \rangle - \langle \omega^{3} \rangle$ not sufficient to determine S

Dynamic structure factor of the UEG:
($\theta = 1$, $r_s = 10$, $N = 34$, $k = 0.63 k_F$)

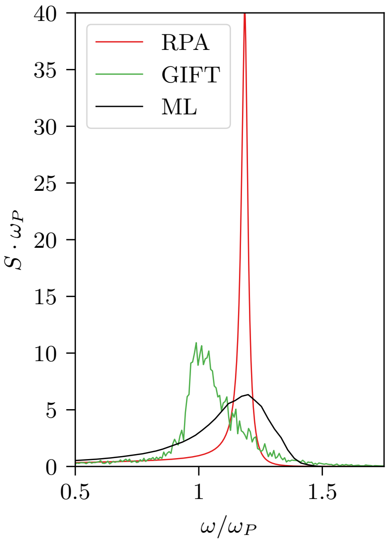

[1] E. Vitali *et al.*, *Phys. Rev. B* **82**, 174510 (2010)

Incorporating additional information on $S(\mathbf{q},\omega)$ via dielectric formulation

- **Fluctuation-dissipation theorem:**

$$S(\mathbf{q},\omega) = -\frac{\mathrm{Im}\chi(\mathbf{q},\omega)}{\pi n(1-e^{-\beta\omega})}$$

Dynamic structure factor of the UEG:
($\theta = 1$, $r_s = 10$, $N = 33$, $q = 0.63 q_F$)

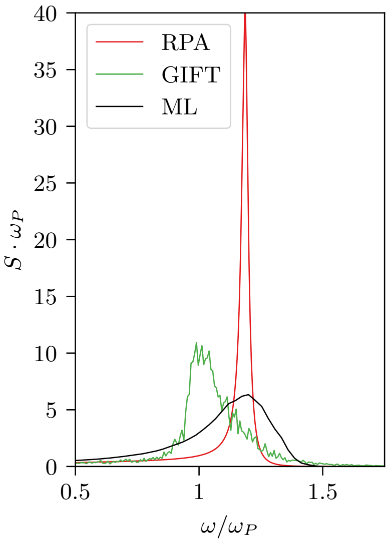

Incorporating additional information on $S(\mathbf{q}, \omega)$ via dielectric formulation

- **Fluctuation-dissipation theorem:**

$$S(\mathbf{q}, \omega) = -\frac{\text{Im}\chi(\mathbf{q}, \omega)}{\pi n(1 - e^{-\beta\omega})}$$

- Express response function χ via ideal response function χ_0 and **dynamic local field correction** G:

$$\chi(\mathbf{q}, \omega) = \frac{\chi_0(\mathbf{q}, \omega)}{1 - v_q \left[1 - G(\mathbf{q}, \omega)\right] \chi_0(\mathbf{q}, \omega)}$$

- **Random phase approximation (RPA):** $G \equiv 0$

Dynamic structure factor of the UEG:
($\theta = 1$, $r_s = 10$, $N = 33$, $q = 0.63 q_F$)

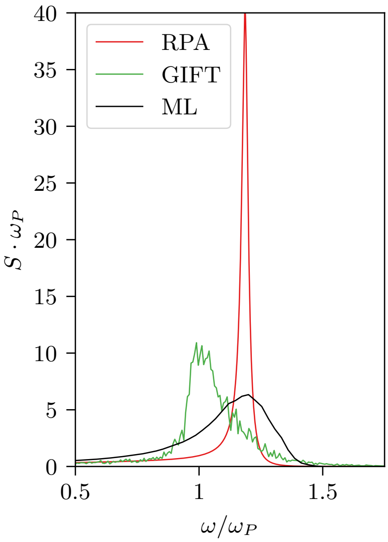

Incorporating additional information on $S(\mathbf{q},\omega)$ via dielectric formulation

- **Fluctuation-dissipation theorem:**

$$S(\mathbf{q},\omega) = -\frac{\mathrm{Im}\chi(\mathbf{q},\omega)}{\pi n(1-e^{-\beta\omega})}$$

- Express response function χ via ideal response function χ_0 and **dynamic local field correction** G:

$$\chi(\mathbf{q},\omega) = \frac{\chi_0(\mathbf{q},\omega)}{1 - v_q\left[1 - G(\mathbf{q},\omega)\right]\chi_0(\mathbf{q},\omega)}$$

- **Random phase approximation (RPA):** $G \equiv 0$

Make ansatz and optimize $G(\mathbf{q},\omega)$ instead of $S(\mathbf{q},\omega)$

Advantages:

- Limits $G(\mathbf{q},0)$ and $G(\mathbf{q},\infty)$ known from PIMC simulation
- Other exact properties of G can be incorporated

Dynamic structure factor of the UEG:
($\theta = 1$, $r_s = 10$, $N = 33$, $q = 0.63q_F$)

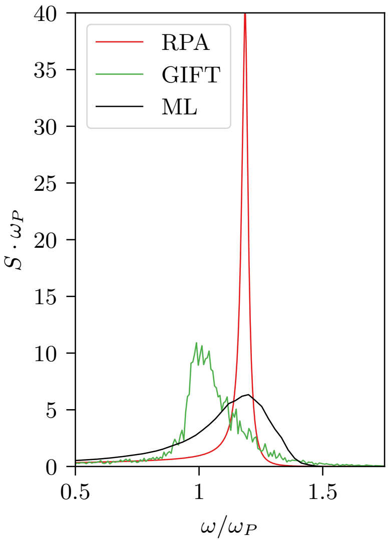

Incorporating additional information on $S(\mathbf{q},\omega)$ via dielectric formulation

- **Fluctuation-dissipation theorem:**

$$S(\mathbf{q},\omega) = -\frac{\mathrm{Im}\chi(\mathbf{q},\omega)}{\pi n(1-e^{-\beta\omega})}$$

- Express response function χ via ideal response function χ_0 and **dynamic local field correction** G:

$$\chi(\mathbf{q},\omega) = \frac{\chi_0(\mathbf{q},\omega)}{1 - v_q\left[1-G(\mathbf{q},\omega)\right]\chi_0(\mathbf{q},\omega)}$$

- **Random phase approximation (RPA):** $G \equiv 0$

Make ansatz and optimize $G(\mathbf{q},\omega)$ instead of $S(\mathbf{q},\omega)$

Advantages:

- Limits $G(\mathbf{q},0)$ and $G(\mathbf{q},\infty)$ known from PIMC simulation
- Other exact properties of G can be incorporated

Dynamic structure factor of the UEG:
($\theta = 1$, $r_s = 10$, $N = 33$, $q = 0.63q_F$)

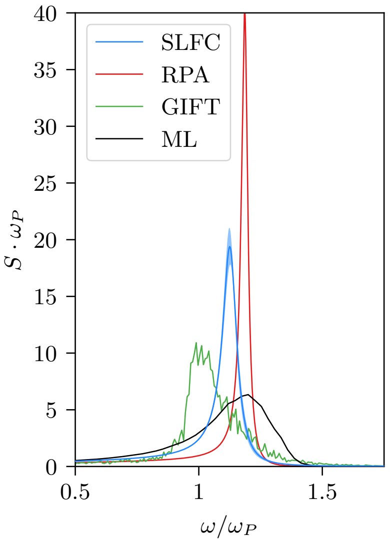

Incorporating additional information on $S(\mathbf{q},\omega)$ via dielectric formulation

- **Fluctuation-dissipation theorem:**

$$S(\mathbf{q},\omega) = -\frac{\text{Im}\chi(\mathbf{q},\omega)}{\cdots}$$

- Ex
dy

GIFT and ML spectra not in agreement with exact properties of $G(\mathbf{q},\omega)$
$\rightarrow$ to be discarded as unphysical

$$\chi(\mathbf{q},\omega) = \frac{\cdots}{1 - v_q\left[1 - G(\mathbf{q},\omega)\right]\chi_0(\mathbf{q},\omega)}$$

- **Random phase approximation (RPA):** $G \equiv 0$

Make ansatz and optimize $G(\mathbf{q},\omega)$ instead of $S(\mathbf{q},\omega)$

Advantages:

- Limits $G(\mathbf{q},0)$ and $G(\mathbf{q},\infty)$ known from PIMC simulation
- Other exact properties of G can be incorporated

Dynamic structure factor of the UEG:
$(\theta = 1, r_s = 10, N = 33, q = 0.63 q_F)$

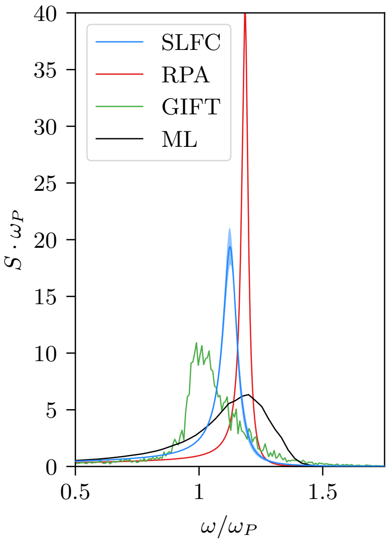

Incorporating additional information on $S(\mathbf{q}, \omega)$ via dielectric formulation

- **Fluctuation-dissipation theorem:**

$$S(\mathbf{q}, \omega) = -\frac{\mathrm{Im}\chi(\mathbf{q}, \omega)}{\ldots}$$

- Ex... dy...

GIFT and ML spectra not in agreement with exact properties of $G(\mathbf{q}, \omega)$ $\rightarrow$ to be discarded as unphysical

$$\chi(\mathbf{q}, \omega) = \frac{\ldots}{1 - v_q\left[1 - G(\mathbf{q}, \omega)\right]\chi_0(\mathbf{q}, \omega)}$$

- **Random phase approximation (RPA):** $G \equiv 0$

Stochastic sampling of $G(\mathbf{q}, \omega)$ accurately determines $S(\mathbf{q}, \omega)$

Advantages:

- Limits $G(\mathbf{q}, 0)$ and $G(\mathbf{q}, \infty)$ known from PIMC simulation
- Other exact properties of G can be incorporated

Dynamic structure factor of the UEG:
($\theta = 1$, $r_s = 10$, $N = 33$, $q = 0.63q_F$)

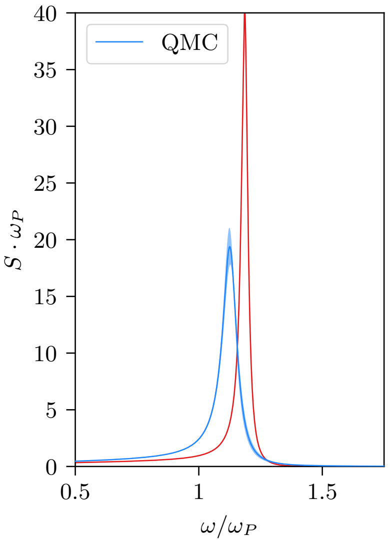

Correlation effects in the dispersion relation: $\theta = 1$, $r_s = 2$

T. Dornheim, S. Groth, J. Vorberger, and M. Bonitz, *Phys. Rev. Lett.* **121**, 255001 (2018)

- Slight **correlation induced redshift** for intermediate q (at small r_s)

Dynamic structure factor of the UEG:

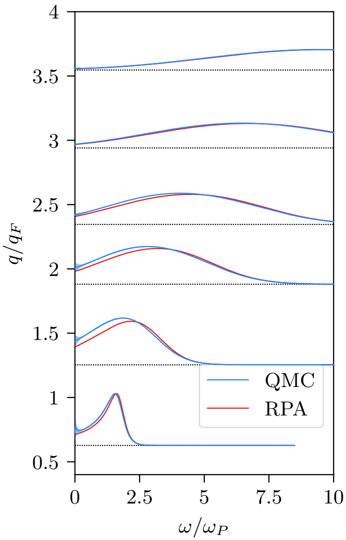

Peak position and FWHM:

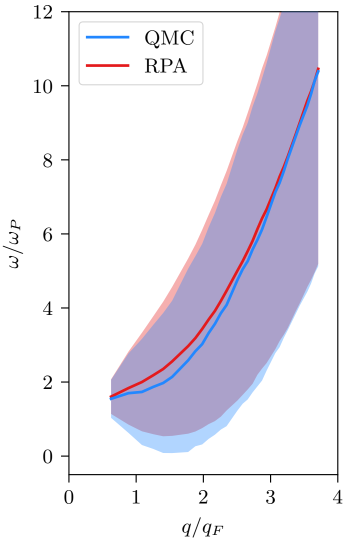

Correlation effects in the dispersion relation: $\theta = 1$, $r_s = 6$

T. Dornheim, S. Groth, J. Vorberger, and M. Bonitz, *Phys. Rev. Lett.* **121**, 255001 (2018)

- Slight **correlation induced redshift** for intermediate q (at small r_s)
- **Pronounced redshift** and **broadening** with increasing r_s

Dynamic structure factor of the UEG:

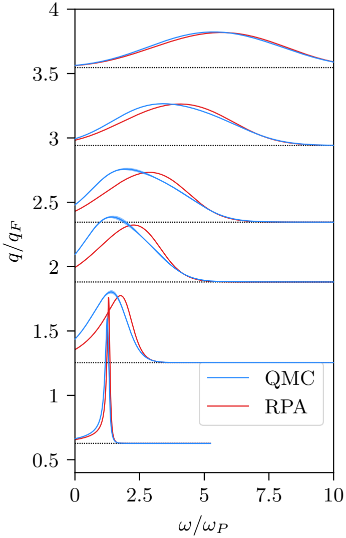

Peak position and FWHM:

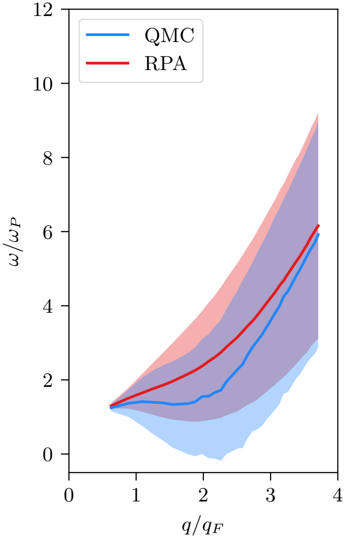

Correlation effects in the dispersion relation: $\theta = 1$, $r_s = 10$

T. Dornheim, S. Groth, J. Vorberger, and M. Bonitz, *Phys. Rev. Lett.* **121**, 255001 (2018)

- Slight **correlation induced redshift** for intermediate q (at small r_s)
- **Pronounced redshift** and **broadening** with increasing r_s
- **Negative plasmon dispersion** for large r_s around $q = 2q_F$ **predicted for dense hydrogen**
- **dispersion** and $S(q,\omega)$ serve as rigorous benchmark for models

Dynamic structure factor of the UEG:

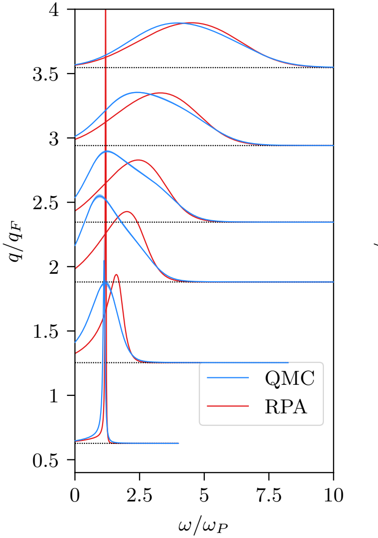

Peak position and FWHM:

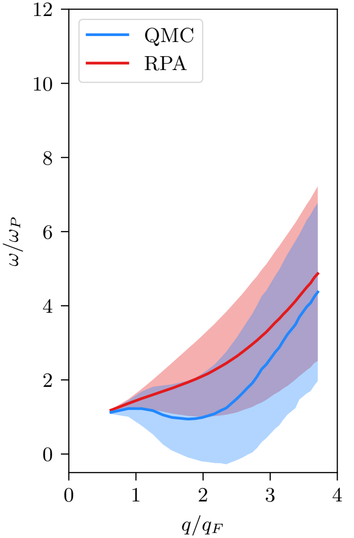

Temperature effects in the dynamic structure factor at $r_s = 10$

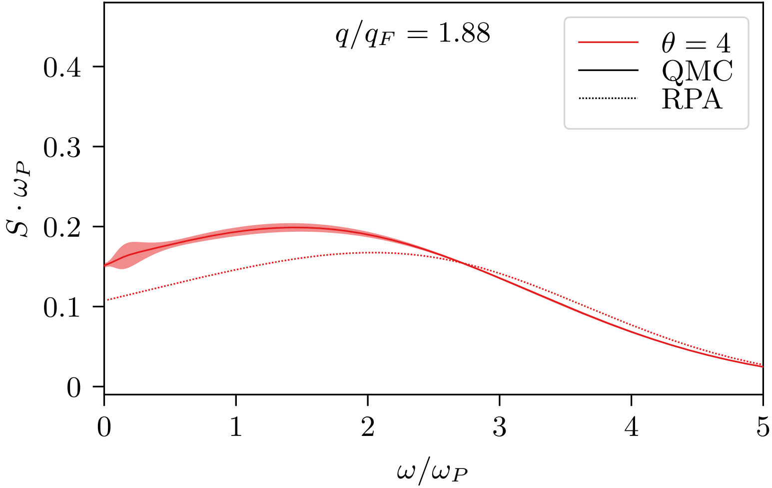

Temperature effects in the dynamic structure factor at $r_s = 10$

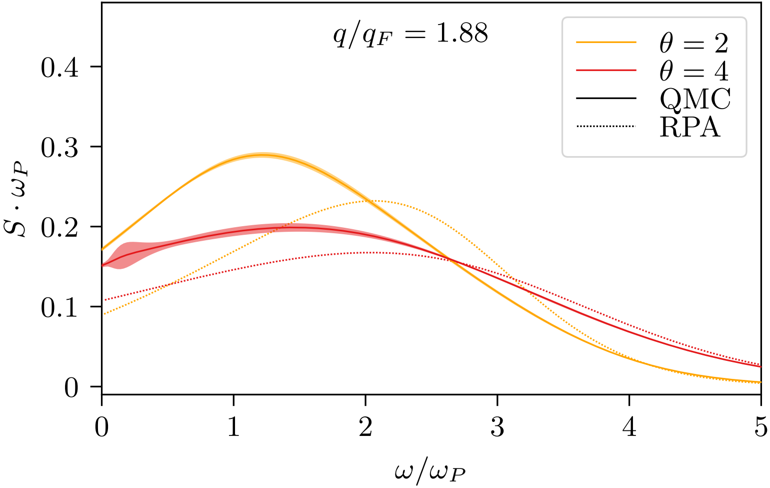

Temperature effects in the dynamic structure factor at $r_s = 10$

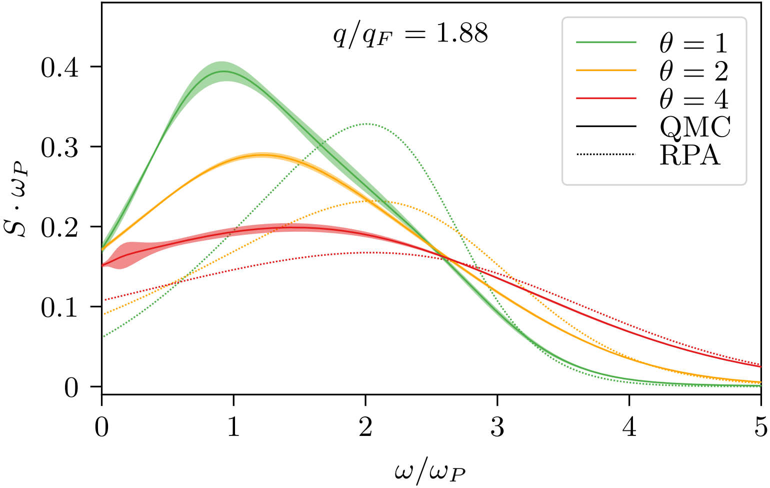

Temperature effects in the dynamic structure factor at $r_s = 10$

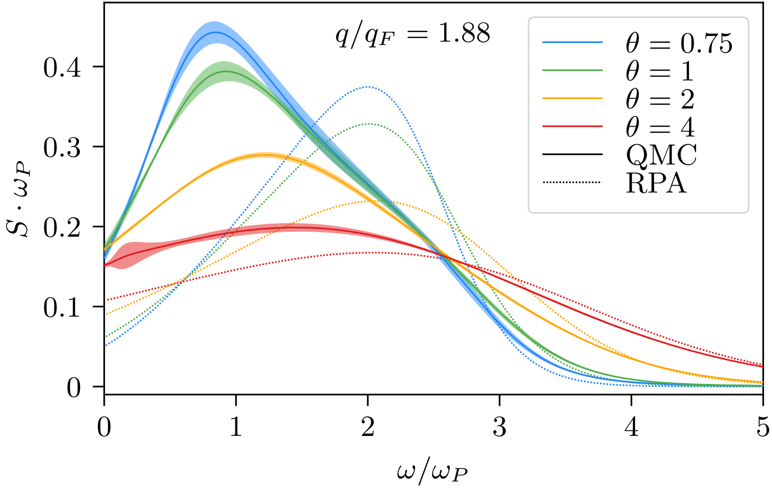

Manifestation of non-trivial shapes in $S(\mathbf{q}, \omega)$ towards low T

The Static Local Field Correction: *Ab initio* PIMC Simulations

- PIMC gives direct access to imaginary-time density–density correlation function:

$$F(\mathbf{q},\tau) = \frac{1}{N}\langle\rho(\mathbf{q},\tau)\rho(-\mathbf{q},0)\rangle$$

Source: S. Groth, **TD**, and J. Vorberger, *Phys. Rev. B* **99**, 235122 (2019)

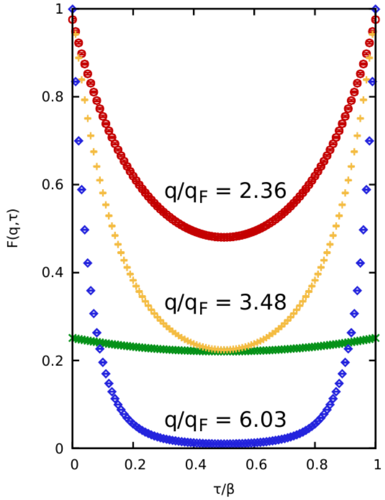

The Static Local Field Correction: *Ab initio* PIMC Simulations

- PIMC gives direct access to imaginary-time density–density correlation function:

$$F(\mathbf{q},\tau) = \frac{1}{N}\left\langle \rho(\mathbf{q},\tau)\rho(-\mathbf{q},0)\right\rangle$$

- $F(\mathbf{q},\tau)$ is directly connected to **static** density response $\chi(\mathbf{q}) = \chi(\mathbf{q},\omega=0)$:

$$\chi(\mathbf{q}) = -n\int_0^\beta \mathrm{d}\tau\ F(\mathbf{q},\tau)$$

$\rightarrow$ Full **q**-dependence from a single simulation of the **unperturbed UEG**

Source: S. Groth, **TD**, and J. Vorberger, *Phys. Rev. B* **99**, 235122 (2019)

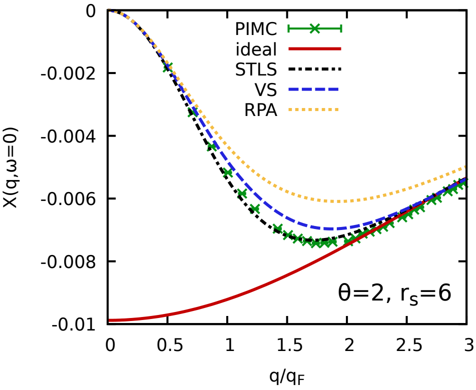

The Static Local Field Correction: *Ab initio* PIMC Simulations

- PIMC gives direct access to imaginary-time density–density correlation function:

$$F(\mathbf{q},\tau) = \frac{1}{N}\langle\rho(\mathbf{q},\tau)\rho(-\mathbf{q},0)\rangle$$

- $F(\mathbf{q},\tau)$ is directly connected to **static** density response $\chi(\mathbf{q}) = \chi(\mathbf{q},\omega=0)$:

$$\chi(\mathbf{q}) = -n\int_0^\beta \mathrm{d}\tau\ F(\mathbf{q},\tau)$$

$\rightarrow$ Full **q**-dependence from a single simulation of the **unperturbed UEG**

- $G(q)$ can be obtained as the deviation from $\chi_0(q)$:

$$G(\mathbf{q}) = 1 - \frac{1}{v_q}\left(\frac{1}{\chi_0(\mathbf{q},0)} - \frac{1}{\chi(\mathbf{q})}\right) \quad .$$

Source: S. Groth, **TD**, and J. Vorberger, *Phys. Rev. B* **99**, 235122 (2019)

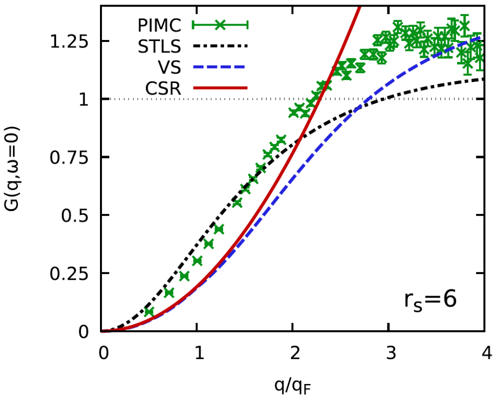

The Static Local Field Correction: Neural-net representation

Extensive set of new PIMC data

- QMC data available at discrete grid (q; θ, r_s)

Source: T. Dornheim *et al.*, J. Chem. Phys. (2019)

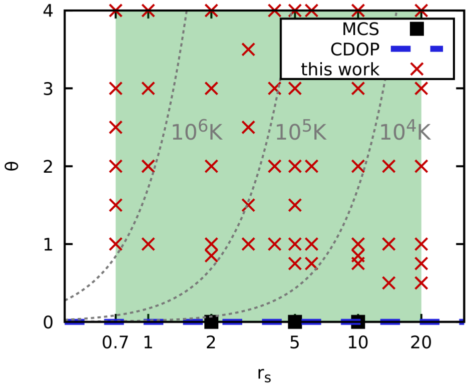

The Static Local Field Correction: Neural-net representation

Extensive set of new PIMC data

- QMC data available at discrete grid (q; θ, r_s)
- **Problem:** Applications (DFT, hydrodynamics, . . .) typically require continuous representation

Source: T. Dornheim *et al.*, J. Chem. Phys. (2019)

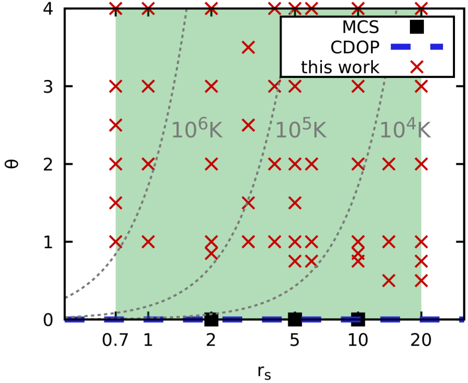

The Static Local Field Correction: Neural-net representation

Extensive set of new PIMC data

Source: T. Dornheim *et al.*, J. Chem. Phys. (2019)

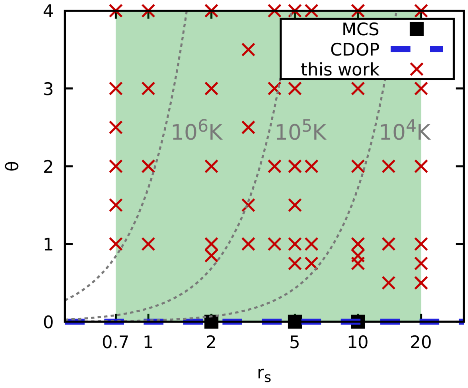

- QMC data available at discrete grid $(q; \theta, r_s)$
- **Problem:** Applications (DFT, hydrodynamics, . . .) typically require continuous representation
- Complicated, non-trivial behavior of $G(q; r_s, \theta)$, only few analytical limits are known

The Static Local Field Correction: Neural-net representation

Extensive set of new PIMC data

- QMC data available at discrete grid (q; θ, r_s)
- **Problem:** Applications (DFT, hydrodynamics, . . .) typically require continuous representation
- Complicated, non-trivial behavior of $G(q; r_s, \theta)$, only few analytical limits are known
- **Solution:** Neural net as flexible function approximator

Source: T. Dornheim *et al.*, J. Chem. Phys. (2019)

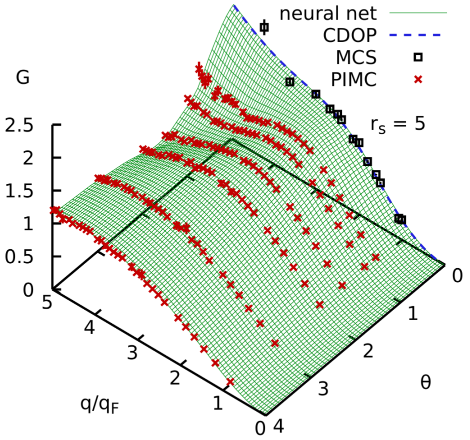

The Static Local Field Correction: Neural-net representation

Extensive set of new PIMC data

- QMC data available at discrete grid (q; θ, r_s)
- **Problem:** Applications (DFT, hydrodynamics, . . .) typically require continuous representation
- Complicated, non-trivial behavior of $G(q; r_s, \theta)$, only few analytical limits are known
- **Solution:** Neural net as flexible function approximator
- **Successful validation against independent data!**
- **Basis for transport quantities, screened ion potential**
  Benchmarks for models and simulations

Source: T. Dornheim *et al.*, J. Chem. Phys. (2019)

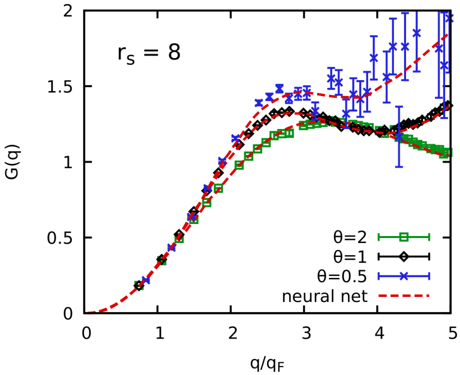

The Static Local Field Correction: Neural-net representation

Extensive set of new PIMC data

Source: T. Dornheim *et al.*, J. Chem. Phys. (2019)

- QMC data available at discrete grid (q; θ, r_s)
- **Problem:** Applications (DFT, hydrodynamics, . . .) typically requir
- Comp analyt
- **Solution:** Neural net as flexible function approximator
- **Successful validation against independent data!**
- **Basis for transport quantities, screened ion potential**
  Benchmarks for models and simulations

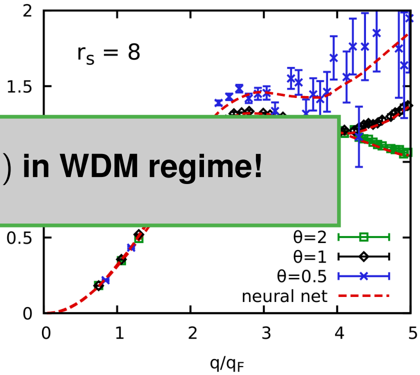

Complete *ab initio* data for $G(q; r_s, \theta)$ in WDM regime!

Part II: Warm dense matter out of equilibrium

- **increasing experimental relevance**:
  femtosecond pump-probe experiments with lasers and free electron lasers:
  XFEL (Hamburg), LCLS (Stanford), China
  e.g. A. Ng, S. Glenzer

- **Theoretical approaches**

  1. Quantum kinetic theory[4], nonequilibrium Green functions[5]: Gericke *et al.*, Vorberger *et al.*, Bornath *et al.*
     new simulations currently being developed in Kiel (WDM conference 2019)
  2. Time-dependent DFT (TD-DFT), e.g. A. Baczewski *et al.*
  3. (Quantum) Hydrodynamics

---

[4] M. Bonitz, "Quantum Kinetic Theory", 2nd ed., Springer 2016
[5] D. Kremp *et al.*, "Quantum Statistics of Nonideal Plasmas", Springer 2005

Nonequilibrium Green functions approach to the dynamical structure factor

VOLUME 84, NUMBER 8 PHYSICAL REVIEW LETTERS 21 FEBRUARY 2000

Real-Time Kadanoff-Baym Approach to Plasma Oscillations in a Correlated Electron Gas

N.-H. Kwong* and M. Bonitz
Fachbereich Physik, Universität Rostock, Universitätsplatz 3, D-18051 Rostock, Germany
(Received 30 August 1999)

A nonequilibrium Green's functions approach to the collective response of correlated Coulomb systems at finite temperatures is presented. It is shown that solving Kadanoff-Baym-type equations of motion for the two-time correlation functions including the external perturbing field allows one to compute the plasmon spectrum with collision effects in a systematic and consistent way. The scheme has a "built-in" sum-rule preservation and is simpler to implement numerically than the equivalent equilibrium approach based on the Bethe-Salpeter equation.

PACS numbers: 73.20.Mf, 05.30.−d

- Relation to equilbrium approaches: M. Bonitz, "Quantum Kinetic Theory", 2nd ed., Springer (2016)
- Similar approach in TD-DFT (Bertsch, Yabana 1995)

Nonequilibrium Green functions approach to the dynamical structure factor

VOLUME 84, NUMBER 8 PHYSICAL REVIEW LETTERS 21 FEBRUARY 2000

Real-Time Kadanoff-Baym Approach to Plasma Oscillations in a Correlated Electron Gas

N.-H. Kwong* and M. Bonitz
Fachbereich Physik, Universität Rostock, Universitätsplatz 3, D-18051 Rostock, Germany
(Received 30 August 1999)

A nonequilibrium Green's functions approach to the collective response of correlated Coulomb systems at finite temperatures is presented. It is shown that solving Kadanoff-Baym-type equations of motion for the two-time correlation functions including the external perturbing field allows one to compute the plasmon spectrum with collision effects in a systematic and consistent way. The scheme has a "built-in" sum-rule preservation and is simpler to implement numerically than the equivalent equilibrium approach based on the Bethe-Salpeter equation.

PACS numbers: 73.20.Mf, 05.30.−d

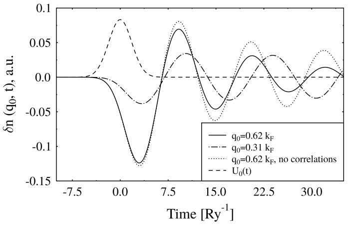

FIG. 1. Density fluctuation of a strongly correlated electron gas for two wave numbers. For comparison, the uncorrelated response for one wave number (dotted line) and the exciting field (dashes) are shown, too. k_F denotes the Fermi momentum, Ry = 13.6 eV.

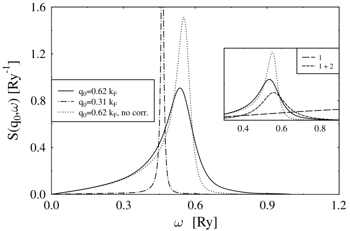

FIG. 2. Dynamic structure factor (12) for the correlated electron gas of Fig. 1 (same line styles). Inset shows S for $q_0 = 0.62k_F$ and contains two other approximations to the correlations corresponding to retaining the first diagram in Eq. (17) and first plus second diagrams, respectively.

Quantum hydrodynamics (QHD) for plasmas: problems and open questions

- **Examples of quantum fluid theories**
  - Fermi liquid theory (Landau, Abrikosov...): metals, quasiparticles non-Fermi liquids (Luttinger)
  - quantum spin liquids (magnetic materials); superfluid theory (Bogolyubov)
- **kinetic theory approach**: moments of the momentum distribution function:
  $n \sim \langle v^0 \rangle, \quad \mathbf{u} \sim \langle \mathbf{v}^1 \rangle, \quad P \sim \langle \mathbf{v}\mathbf{v} \rangle$ etc. $\Rightarrow$ hierarchy of moment equations
  - a) truncation of the moment hierarchy (phenomenological closure)
  - b) asymptotic schemes, small parameter, e.g. $\epsilon = \lambda_{\rm mfp}/L \ll 1$,
    $f(\mathbf{r}, \mathbf{v}, t) = f_0(\mathbf{r}, \mathbf{v}, t) + \epsilon f_1(\mathbf{r}, \mathbf{v}, t) + \ldots$
    $f_0(\mathbf{r}, \mathbf{v}, t) = n(\mathbf{r}, t) \left(\frac{m}{2\pi k_B T(\mathbf{r}, t)} \right)^{3/2} \exp \left[\frac{m(\mathbf{v} - \mathbf{u}(\mathbf{r}, t))^2}{2k_B T(\mathbf{r}, t)} \right],$
    f_0: collision integrals vanish $\Rightarrow$ no heat flux, no viscous stress
    f_1 expanded into Laguerre/Sonine polynomials (Chapman-Enskog)
- **no similar mature approaches to quantum plasmas**, except for linear response theory (Zubarev, Röpke, ... generalized Gibbs ensemble)

QHD for plasmas: problems and open questions

Quantum hydrodynamics – status:

- straightforward for a single particle and for bosons
- fermions, plasmas: questionable assumptions in derivation[a]
- In many papers: incorrect coefficients in QHD equations[b]

questionable predictions:

- “novel attractive forces” between ions in quantum plasmas[c]
- “spinning quantum plasmas”,
- most recent example: “quantum dusty plasmas” (see figure)[d]

questionable claims of relevance:

- semiconductors, metals
- white dwarfs, magnetars, neutron stars

Are they sure?? Can they prove it??
how important are solitons in neutron starts??

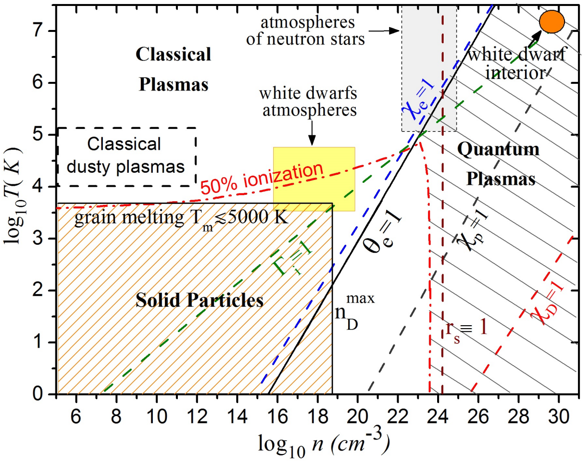

[a]Manfredi, Haas, PRB 2001

[b]*clarification:* Michta, Graziani, Bonitz, Contrib. Plasma Phys. **55**, 437 (2015), Moldabekov *et al.*, Phys. Plasmas **25**, 031903 (2018), *open access*

[c]Shukla, Eliasson, PRL **108**, 165007 (2012); *correction:* Bonit *et al.*, PRE **87**, 033105 (2013), Moldabekov *et al.*, Phys. Plasmas (2015)

[d]Shukla, Ali, Phys. Plasmas **12**, 114502 (2005); *clarification*: Bonitz, Moldabekov, Ramazanov, Phys. Plasmas **26**, 090601 (2019), *perspectives article, Editors’ pick, open access*

QHD for plasmas: advancing quantum plasma research

Contributions to Plasma Physics CPP

enforce high quality standards: manuscripts should[6]

1. present an important **advance to plasma physics**;
2. contain a **convincing motivation** of the research in the introduction explaining the importance of the work;
3. present **applications to concrete plasmas** (in case of experiments) and—in case of theory—**clear predictions for real plasmas**, including their physical parameters;
4. not be purely formal studies of mathematical properties of equations, for example, in terms of dimensionless parameters, without application to real plasmas, as discussed in 3.

[6] M. Bonitz, Editorial: Contrib. Plasma Phys. **59** (1), 8 (2019)

Fluid description of quantum dynamics

- N interacting identical quantum particles, hamiltonian

$$\hat{H} = \sum_{i=1}^{N}\left(-\frac{\hbar^2}{2m}\nabla_i^2 + V(\mathbf{r}_i)\right) + \frac{1}{2}\sum_{i\neq j} w_{ij}(\mathbf{R}),$$

  $\mathbf{R} = (\mathbf{r}_1, \sigma_1; \mathbf{r}_2, \sigma_2; \dots \mathbf{r}_N, \sigma_N)$, $\mathbf{r}_i$ are the particle coordinates and σ_i their spin projections.

- for a pure state: dynamics governed by the **N-particle Schrödinger equation**

$$i\hbar\frac{\partial\Psi(\mathbf{R},t)}{\partial t} = \hat{H}\Psi(\mathbf{R},t), \quad \Psi(\mathbf{R},t_0) = \Psi_0(\mathbf{R})\,,$$

  normalization: $\sum_{\sigma_1\dots\sigma_N}\int d^{3N}R\,|\Psi(\mathbf{R},t)|^2 = N$,
  for particles with spin s: $g_s = 2s+1$ different spin projections

- ansatz with **real amplitude and phase** (Bohm, Madelung)[7]:

$$\Psi(\mathbf{R},t) = A(\mathbf{R},t)\,e^{\frac{i}{\hbar}S(\mathbf{R},t)}, \qquad A, S \in \mathcal{R}\,.$$

- can be used for semiclassical molecular dynamics, e.g. Gericke, Gregori *et al.* (2018)

---

[7] E. Madelung, Z. Phys. (1927), D. Bohm, Phys. Rev. (1952)

Quantum hydrodynamics for 1 particle

hydrodynamic fields from wave function (for pure state):

$$n(\mathbf{r},t) = A^2(\mathbf{r},t), \qquad \text{density},$$
$$\mathbf{p}(\mathbf{r},t) = m\mathbf{v}(\mathbf{r},t) = \nabla S(\mathbf{r},t), \qquad \text{momentum},$$

exact “hydrodynamic” equations:

$$\frac{\partial n}{\partial t} + \nabla(\mathbf{v}n) = 0,$$
$$\frac{\partial \mathbf{p}}{\partial t} + \mathbf{v}\nabla\mathbf{p} = -\nabla(V+Q),$$
$$Q[n(\mathbf{r},t)] = -\frac{\hbar^2}{2m}\frac{\nabla^2 n^{1/2}}{n^{1/2}}\,, \qquad \text{“Bohm potential''},$$

Modifications for N fermions:

- spin statistics (Pauli principle): N different orbitals $\phi_i \Rightarrow$ different $n_i, \mathbf{p}_i$
- interaction w_{ij} between particles
- statistical weight f_i of each orbital?
- coupling of orbitals? Definition of mean n and $\mathbf{p}$?

Statistical description of N-particle quantum system[8]

- mixed state described by *N*-**particle density operator**:

$$\hat{\rho}(t) = \sum_a p_a |\Psi^a(t)\rangle\langle\Psi^a(t)| \,, \quad \mathrm{Tr}\, \hat{\rho}(t) = 1 \,,$$

  sum over projection operators on all solutions of the Schrödinger equation,
  p_a: real probabilities, $0 \le p_a \le 1$, with $\sum_a p_a = 1$
- **one-particle reduced density operator**:

$$\hat{F}_1(t) \equiv N \mathrm{Tr}_{2\ldots N} \hat{\rho}(t) \,, \quad \mathrm{Tr}_1 \hat{F}_1 = N \,.$$

- equation of F_1: **quantum kinetic equation**, $\hat{F}_{12} = \hat{F}_1 \hat{F}_2 + \hat{g}_{12}$:

$$i\hbar \frac{\partial \hat{F}_1}{\partial t} - [\hat{\bar{H}}_1, \hat{F}_1] = \mathrm{Tr}_2[\hat{w}_{12}, \hat{g}_{12}] \equiv \hat{I}_1[\hat{g}_{12}], \quad \text{collision integral} \,,$$

$$\hat{\bar{H}}_1(t) = \hat{H}_1 + \hat{H}_1^{\mathrm{H}}(t), \quad \hat{H}_1^{\mathrm{H}}(t) \equiv \mathrm{Tr}_2 \hat{w}_{12} \hat{F}_2(t), \quad \text{mean field} \,,$$

[8] M. Bonitz, “Quantum Kinetic Theory”, 2nd ed., Springer 2016

Density matrix equation in Hartree approximation

- **mean field approximation** (no anti-symmetrization, no correlations):

$$\Psi(\mathbf{R}, t) \approx \phi_{\alpha_1}(\mathbf{r}_1) \cdot \phi_{\alpha_2}(\mathbf{r}_2) \cdot \dots \cdot \phi_{\alpha_N}(\mathbf{r}_N), \quad \langle \phi_\alpha | \phi_\beta \rangle = \delta_{\alpha,\beta}$$

$\phi_{\alpha_k}(\mathbf{r}_k)$: single-particle orbital occupied by particle k,

for density operators: no antisymmetrization and $\hat{I}_1 = 0 \Rightarrow \hat{F}_{12} \approx \hat{F}_1 \hat{F}_2$

- **coordinate representation**: $\langle \mathbf{r}' | \hat{F}_1(t) | \mathbf{r}'' \rangle = f(\mathbf{r}', \mathbf{r}'', t), \quad \text{density} \quad \text{matrix}$

$$\begin{aligned}
i\hbar \frac{\partial}{\partial t} f(\mathbf{r}', \mathbf{r}'', t) &= -\frac{\hbar^2}{2m} \left(\nabla^2_{r'} - \nabla^2_{r''} \right) f(\mathbf{r}', \mathbf{r}'', t) \\
&\quad + \left\{ U^{\rm eff}(\mathbf{r}', t) - U^{\rm eff}(\mathbf{r}'', t) \right\} f(\mathbf{r}', \mathbf{r}'', t) \\
U^{\rm eff}(\mathbf{r}, t) &= V(\mathbf{r}, t) + U^{\rm H}(\mathbf{r}, t), \\
U^{\rm H}(\mathbf{r}, t) &= g_s \int d\bar{r}\, w(r - \bar{r})\, f(\bar{r}, \bar{r}, t),
\end{aligned}$$

diagonal element of the density matrix: $f(\mathbf{r}, \mathbf{r}, t) = n(\mathbf{r}, t)$, density

Hartree approximation for fermions

- **mean field approximation** (no anti-symmetrization, no correlations):

$$\Psi(\mathbf{R}, t) \approx \phi_{\alpha_1}(\mathbf{r}_1) \cdot \phi_{\alpha_2}(\mathbf{r}_2) \cdots \cdot \phi_{\alpha_N}(\mathbf{r}_N), \quad \langle \phi_\alpha | \phi_\beta \rangle = \delta_{\alpha,\beta}$$

  Thermodynamic equilibrium: orbitals $\phi_1, \phi_2 \dots$ occupied with probability $f_i = [e^{\beta(\epsilon_i - \mu)} + 1]^{-1}, \quad i = 1 \dots \infty$

- One-particle density operator and density matrix:

$$\hat{F}_1 = N \, \mathrm{Tr}_{2\dots \mathrm{N}} \sum_\alpha \frac{1}{\mathrm{Z_G}} \mathrm{e}^{-\beta(\mathrm{E}_\alpha - \mu \mathrm{N}_\alpha)} \, |\psi_\alpha\rangle\langle\psi_\alpha| = \mathrm{N} \sum_{\mathrm{i}=1}^{\infty} \mathrm{f_i} \, |\phi_\mathrm{i}\rangle\langle\phi_\mathrm{i}|$$

$$f(\mathbf{r}', \mathbf{r}'', t) = N \sum_{i=1}^{\infty} f_i \, \phi_i(\mathbf{r}', t) \phi_i^*(\mathbf{r}'', t) \,,$$

- Equation for f solved by set of nonlinear “Hartree-”Schrödinger (t-dependent Kohn-Sham) equations:

$$i\hbar \frac{\partial}{\partial t} \phi_i(\mathbf{r}, t) = \left\{ -\frac{\hbar^2}{2m} \nabla_\mathbf{r}^2 + V(\mathbf{r}, t) + U_F^{\mathrm{H}}(\mathbf{r}, t) \right\} \phi_i(\mathbf{r}, t) \,,$$

$$U_F^{\mathrm{H}}[n(\mathbf{r}, t)] = \int d\mathbf{r}_2 \, w(\mathbf{r} - \mathbf{r}_2)[g_s n(\mathbf{r}_2, t) - n_0],$$

U_F^{H} : Hartree mean field, $n(\mathbf{r}, t) = \sum_{i=1}^{\infty} f_i \, |\phi_i(\mathbf{r}, t)|^2$. n_0: background

Microscopic QHD equations (MQHD)[10]

- in TDSE: introduce real amplitude ($A_i = n_i^{1/2}$) and phase for each orbital:
- restore exchange-correlation effects formally exactly[9]: *either*
  i) potential $V^{\rm xc} = V^{\rm xc}[n(\mathbf{r}, \tilde{t})]$, from TD-DFT, *or, alternatively,*
  ii) collision integral $I_i[g_{12}(\tilde{t})]$ from quantum kinetic theory

$$
\begin{aligned}
\frac{\partial n_i}{\partial t} + \nabla(\mathbf{v}_i n_i) &= 0, \\
\frac{\partial \mathbf{p}_i}{\partial t} + \mathbf{v}_i \mathrm{div} \mathbf{p}_i &= -\nabla \left(V(\mathbf{r}, t) + U^{\rm H} + Q_i + V^{\rm xc} + I_i \right) , \\
U^{\rm H}[n(\mathbf{r}, t)] &= \int d\mathbf{r}_2 \, w(\mathbf{r} - \mathbf{r}_2)[g_s n(\mathbf{r}_2, t) - n_0], \\
Q_i(\mathbf{r}, t) &= -\frac{\hbar^2}{2m} \frac{\nabla^2 \sqrt{n_i(\mathbf{r}, t)}}{\sqrt{n_i(\mathbf{r}, t)}} .
\end{aligned}
$$

- $n(\mathbf{r}, t) = \sum_{i=1}^{\infty} f_i \cdot |\phi_i(\mathbf{r}, t)|^2$, f_i statistical weight (Fermi function), $g_s = 2s + 1$.
- $\Rightarrow$ exact formulation of the many-body problem (with proper set of orbitals), equivalent to TD-DFT

---

[9] in general: memory effects (non-adiabatic), i.e. $t_0 \le \tilde{t} \le t$

[10] Bonitz *et al.*, Phys. Plasmas **26**, 090601 (2019), agrees with Manfredi, Fields Inst. Comm. 2005

Derivation of QHD equations from MQHD[11]

- consider mean field (Hartree / quantum Vlasov) approximation: $V^{\mathrm{xc}} \equiv I_i \equiv 0$
- average MQHD equations over i with weights f_i
- define hydrodynamic (average) quantities:

$$
\begin{aligned}
\overline{n}(\mathbf{r},t) &= \frac{1}{N}\sum_{i=1}^{\infty} f_i\, n_i(\mathbf{r},t)\,, \\
\overline{\mathbf{p}}(\mathbf{r},t) &= \frac{1}{N}\sum_{i=1}^{\infty} f_i\, \mathbf{p}_i(\mathbf{r},t)\,, \\
\overline{Q}(\mathbf{r},t) &= -\frac{\hbar^2}{2mN}\sum_{i=1}^{\infty} f_i \frac{\nabla^2\sqrt{n_i(\mathbf{r})}}{\sqrt{n_i(\mathbf{r})}} \neq \frac{\hbar^2}{2mN}\frac{\nabla^2\sqrt{\overline{n}(\mathbf{r})}}{\sqrt{\overline{n}(\mathbf{r})}} \equiv Q_1[\overline{n}]\,.
\end{aligned}
$$

- final equality was *postulated* by Manfredi and Haas (PRB 2001, Fields Inst. Comm. 2005) reproducing *single-particle* QHD equations (with Hartree potential)
- When does it hold? What are the corrections? ⇒ perform strict derivation

[11] Bonitz *et al.*, Phys. Plasmas 2019

Derivation of QHD equations (contd.)[12]

- use average of product: $\overline{a_i b_i} = \overline{a} \cdot \overline{b} + \overline{\delta a_i \delta b_i}$,
- result: **formally exact QHD equations** from orbital average of MQHD (TD-DFT):

$$\frac{\partial \overline{n}}{\partial t} + \frac{1}{m}\nabla(\overline{\mathbf{p}} \cdot \overline{n}) = J^{\Delta}_{np}$$

$$\frac{\partial \overline{\mathbf{p}}}{\partial t} + \frac{1}{m}\overline{\mathbf{p}} \cdot \mathrm{div}\overline{\mathbf{p}} = -\nabla \left(V(\mathbf{r}, t) + U^{\mathrm{H}}_F[\overline{n}] + Q_1[\overline{n}] + Q^{\Delta} + V^{\mathrm{xc}}[\overline{n}] \right) + J^{\Delta}_{pp}$$

- three correction terms (correlation functions):

$$J^{\Delta}_{np} = -\frac{1}{m}\nabla\,\overline{\delta \mathbf{p}_i \delta n_i}, \quad Q^{\Delta} \approx \frac{\hbar^2}{2m\overline{n}}\overline{\delta A_i \cdot \nabla^2 \delta A_i} + O\left(\left(\frac{\delta A_i}{\overline{A}}\right)^2\right),$$

$$J^{\Delta}_{pp} = -\frac{1}{m}\overline{\delta \mathbf{p}_i \mathrm{div}\, \delta \mathbf{p}_i} = \frac{1}{\overline{n}}\partial_\beta \overline{P}_{\alpha\beta} = \frac{1}{\overline{n}}\nabla \overline{P}_F + \frac{1}{\overline{n}}\partial_\gamma \overline{\sigma}_{\alpha\gamma}, \quad \gamma \neq \alpha, \quad \overline{\sigma} : \text{stress tensor},$$

- special case: **ideal Fermi gas** of dimension $D = 1, 2, 3$, $T = 0$: $\overline{\sigma}_{\alpha\gamma} \to 0$ and

$$J^{\Delta}_{pp} = \frac{1}{D}\nabla\overline{\delta E_{\mathrm{kin}}} = \frac{m}{2(D+2)}\nabla v_F^2 = \frac{1}{2\overline{n}}\nabla \overline{P}^{\mathrm{id}}.$$

[12] Bonitz *et al.*, Phys. Plasmas 2019

Test case plasma oscillations: linearization of MQHD-equations[13]

- stability conditions without excitation:

$$\partial_t n_{i0} = \partial_t \mathbf{p}_{i0} = \overline{v}_{i0} = 0$$
$$\mathbf{v}_{i0}\,\mathrm{div}\mathbf{p}_{i0} = -\nabla\left(U_0^{\mathrm{H}} + Q_{i0}\right)$$

- monochromatic weak excitation: $V_1^{\mathrm{ext}}(\mathbf{r},t) = \tilde{V}_1^{\mathrm{ext}}\, e^{-i\hat{\omega}t + i\mathbf{qr}}$, where $\hat{\omega} = \omega + i\epsilon,\ \epsilon > 0$
- linearization and Fourier-Laplace transform:

$$n_{i0} \to n_{i0} + n_{i1}\,;\, \mathbf{v}_{i0} \to \mathbf{v}_{i0} + \mathbf{v}_{i1}\ ;$$
$$U_0^{\mathrm{H}} \to U_0^{\mathrm{H}} + U_1^{\mathrm{H}}\,;\, Q_{i0} \to Q_{i0} + Q_{i1}\,, \quad U_1^{\mathrm{eff}} = V_1^{\mathrm{ext}} + U_1^{\mathrm{H}}$$

- density response exactly coincides with random phase approximation (RPA)

$$\tilde{n}_1(\mathbf{q},\hat{\omega}) = \frac{1}{N}\sum_{i=1}^{\infty} f_i\, \tilde{n}_{i1}(\mathbf{q},\hat{\omega}) = \tilde{U}_1^{\mathrm{eff}}(\mathbf{q},\hat{\omega})\tilde{\Pi}_1^R(\mathbf{q},\hat{\omega})$$
$$\tilde{\Pi}_1^R(\mathbf{q},\hat{\omega}) = \frac{1}{N}\sum_{i=1}^{\infty} \frac{f_i}{(\hat{\omega} - \mathbf{q}\mathbf{v}_{i0})^2 - \frac{\hbar^2 q^4}{4m^2}}\,.$$

[13] Bonitz *et al.*, Phys. Plasmas 2019, result agrees with Manfredi, Fields Inst. Comm. 2005

Test case plasma oscillations: linearization of QHD equations[15]

- Hartree approximation, neglect correlation terms
- linearization and Fourier-Laplace transform:

$$\overline{n}_0 \to \overline{n}_0 + \overline{n}_1 \; ; \; \overline{\mathbf{v}}_0 \to \overline{\mathbf{v}}_0 + \overline{\mathbf{v}}_1 \; ; \; U_0^{\mathrm{H}} \to U_0^{\mathrm{H}} + U_1^{\mathrm{H}} \; ;$$

$$Q[\overline{n}] \to -\frac{\hbar^2}{2m} \frac{\nabla^2 \sqrt{\overline{n}_0}}{\sqrt{\overline{n}_0}} + \frac{\hbar^2}{4m} \nabla^2 \sqrt{\overline{n}_1} \, ,$$

$$\overline{P}_0^{\mathrm{id}} \to \frac{2}{D+2} \overline{n}_0 E_F(\overline{n}_0) + \frac{2}{D} \frac{\overline{n}_1}{\overline{n}_0} E_F(\overline{n}_0) \, ,$$

- plasmon dispersion – QHD vs. MQHD (RPA): agreement only in 1D, for $\omega \geq \omega_{pl}$

$$\omega^2_{\mathrm{QHD}}(q) = \omega^2_{pl} + \frac{1}{D} v_F^2 q^2 + \frac{\hbar^2}{4m^2} q^4 ,$$

$$\omega^2_{\mathrm{MQHD}}(q) = \omega^2_{pl} + \frac{3}{D+2} v_F^2 q^2 + (1 - \delta_{2,D}) \frac{\hbar^2}{4m^2} q^4 ,$$

- for $\omega < \omega_{pl}$: Bohm potential Q is factor 9 too big $\Rightarrow$ incorrect acoustic modes and statically screened potential[14]

---

[14] Michta *et al.*, CPP **55**, 437 (2015), Moldabekov *et al.*, Phys. Plasmas **25**, 031903 (2018)

[15] Bonitz *et al.*, Phys. Plasmas **26**, 090601 (2019)

Correction of coefficients in QHD equations[16]

- Comparison to RPA reveals ω- and k-dependence of pressure ($\bar{\alpha}$) and Bohm potential (γ). In addition: dependence on temperature, dimensionality

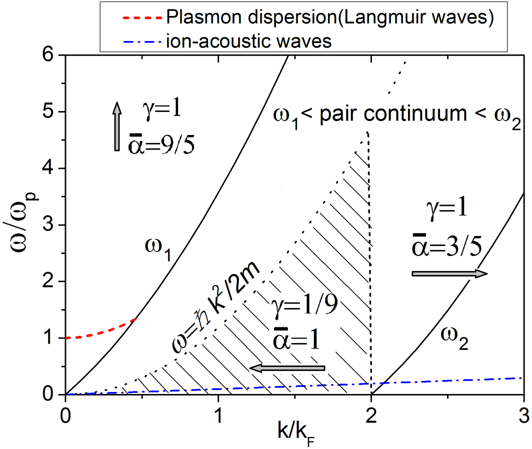

[16] Figure for 3D case, $T = 0$, from: Moldabekov, Bonitz, and Ramazanov, Phys. Plasmas **25**, 031903 (2018)

Summary

- *ab initio* **QMC** simulations provide complete thermodynamic data for warm dense uniform electron gas[17]
- accurate functional $f_{\mathrm{xc}}(r_s, \Theta, \xi)$ input for finite-T LDA-DFT, implemented in Libxc (LDA_XC_GDSMFB)

- ab initio data for inhomogeneous EG[18] $\Rightarrow$ accurate parametrization of static local field correction[19] $G(q)$
- first *ab initio* data for the dynamic structure factor $S(q, \omega)$ of warm dense electrons[20]

[17] T. Dornheim *et al.*, Phys. Reports (2018)
[18] S. Groth *et al.*, J. Chem. Phys. (2017); T. Dornheim *et al.*, Phys. Rev. E (2017)
[19] T. Dornheim et al., J. Chem. Phys. (2019)
[20] T. Dornheim *et al.*, Phys. Rev. Lett. (2018); S. Groth *et al.*, Phy. Rev. B (2019)
[21] Zh. Moldabekov *et al.*, Phys. Plasmas (2018); M. Bonitz *et al.*, Phys. Plasmas (2019)
[22] N. Schlünzen *et al.*, arxiV:1909.11489

Summary

- *ab initio* **QMC** simulations provide complete thermodynamic data for warm dense uniform electron gas[17]
- accurate functional $f_{\mathrm{xc}}(r_s, \Theta, \xi)$ input for finite-T LDA-DFT, implemented in Libxc (LDA_XC_GDSMFB)

- ab initio data for inhomogeneous EG[18] $\Rightarrow$ accurate parametrization of static local field correction[19] $G(q)$
- first *ab initio* data for the dynamic structure factor $S(q, \omega)$ of warm dense electrons[20]

- **QHD** rigorously derived from Microscopic QHD (TDDFT),
  coefficients of Bohm term and pressure depend on excitation conditions [21]
  $\Rightarrow$ systematic improvements possible, promising for large space and time scales in WDM

---

[17] T. Dornheim *et al.*, Phys. Reports (2018)
[18] S. Groth *et al.*, J. Chem. Phys. (2017); T. Dornheim *et al.*, Phys. Rev. E (2017)
[19] T. Dornheim et al., J. Chem. Phys. (2019)
[20] T. Dornheim *et al.*, Phys. Rev. Lett. (2018); S. Groth *et al.*, Phy. Rev. B (2019)
[21] Zh. Moldabekov *et al.*, Phys. Plasmas (2018); M. Bonitz *et al.*, Phys. Plasmas (2019)
[22] N. Schlünzen *et al.*, arxiV:1909.11489

Summary

- *ab initio* **QMC** simulations provide complete thermodynamic data for warm dense uniform electron gas[17]
- accurate functional $f_{\mathrm{xc}}(r_s, \Theta, \xi)$ input for finite-T LDA-DFT, implemented in Libxc (LDA_XC_GDSMFB)

- ab initio data for inhomogeneous EG[18] $\Rightarrow$ accurate parametrization of static local field correction[19] $G(q)$
- first *ab initio* data for the dynamic structure factor $S(q, \omega)$ of warm dense electrons[20]

- **QHD** rigorously derived from Microscopic QHD (TDDFT),
  coefficients of Bohm term and pressure depend on excitation conditions [21]
  $\Rightarrow$ systematic improvements possible, promising for large space and time scales in WDM

- Electronic correlations and correlation build up (thermalization, dynamical screening, Auger processes etc.) are captured by (Nonequilibrium) **Green functions**. Highly efficient new computational techniques available[22]

---

[17] T. Dornheim *et al.*, Phys. Reports (2018)
[18] S. Groth *et al.*, J. Chem. Phys. (2017); T. Dornheim *et al.*, Phys. Rev. E (2017)
[19] T. Dornheim et al., J. Chem. Phys. (2019)
[20] T. Dornheim *et al.*, Phys. Rev. Lett. (2018); S. Groth *et al.*, Phy. Rev. B (2019)
[21] Zh. Moldabekov *et al.*, Phys. Plasmas (2018); M. Bonitz *et al.*, Phys. Plasmas (2019)
[22] N. Schlünzen *et al.*, arxiV:1909.11489

Outlook: simulating WDM out of equilibrium–combination of methods promising

- **QHD** derived via averaging over all orbitals $\phi_\alpha(\mathbf{r}) \Rightarrow$ *no resolution of microscopic lengths scales, $L_A \sim a_B, \lambda_{TF}$, and associated times* $\Rightarrow$ advantage: extendable to large length and time scales

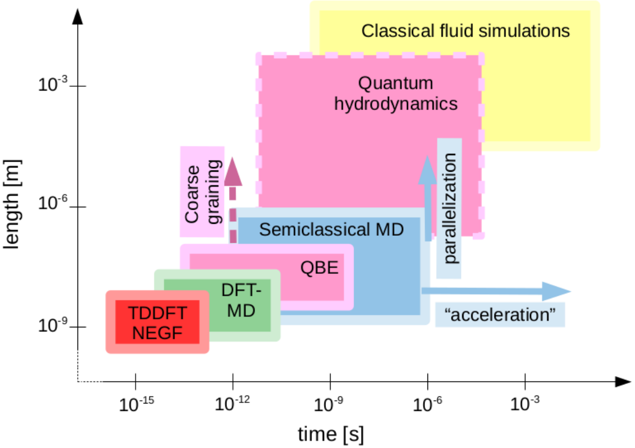

Figure: modified from M. Bonitz *et al.*, *Front. Chem. Science Engin.* (2019); QBE: quantum Boltzmann equation, NEGF: Nonequilibrium Green functions

Outlook: simulating WDM out of equilibrium–combination of methods promising

- **QHD** derived via averaging over all orbitals $\phi_\alpha(\mathbf{r}) \Rightarrow$ *no resolution of microscopic lengths scales,* $L_A \sim a_B, \lambda_{TF}$*, and associated times* $\Rightarrow$ advantage: extendable to large length and time scales
- **DFT-MD** and **TD-DFT** capture atomic scales and inhomogeneity effects. But: miss electronic correlations (inaccurate band gap, ionization energies, no Auger processes etc.)

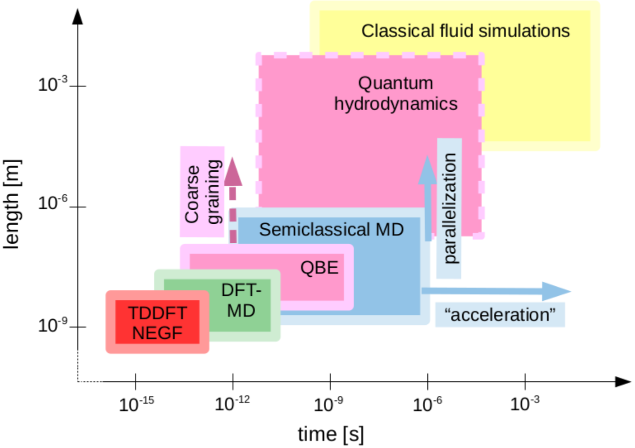

Figure: modified from M. Bonitz *et al.*, *Front. Chem. Science Engin.* (2019); QBE: quantum Boltzmann equation, NEGF: Nonequilibrium Green functions

Outlook: simulating WDM out of equilibrium–combination of methods promising

- **QHD** derived via averaging over all orbitals $\phi_\alpha(\mathbf{r}) \Rightarrow$ *no resolution of microscopic lengths scales, $L_A \sim a_B, \lambda_{TF}$, and associated times* $\Rightarrow$ advantage: extendable to large length and time scales
- **DFT-MD** and **TD-DFT** capture atomic scales and inhomogeneity effects. But: miss electronic correlations (inaccurate band gap, ionization energies, no Auger processes etc.)
- **Green functions, quantum kinetic theory** capture electronic correlations, correlation build up and electron thermalization

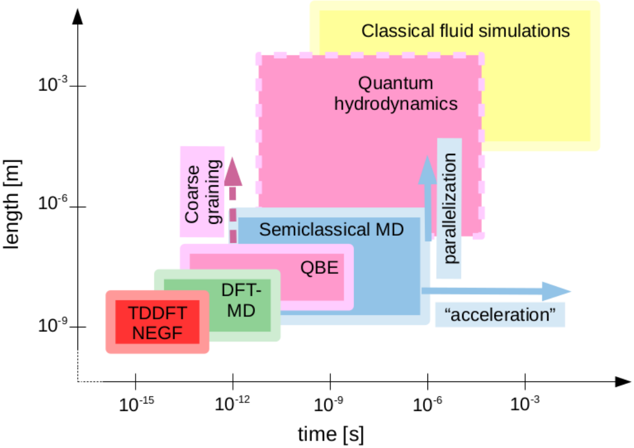

Figure: modified from M. Bonitz *et al.*, *Front. Chem. Science Engin.* (2019); QBE: quantum Boltzmann equation, NEGF: Nonequilibrium Green functions

Outlook: Exciting developments in Warm Dense Matter are ahead of us

Experimental progress requires ambitious theory and simulations
Looking forward to great contributions from Indian plasma physics!

- **Extreme and exotic state of matter:**
  $\rightarrow$ High temperature: $T \sim 10^4 - 10^8\ K$
  $\rightarrow$ Solid state density: $n \sim 10^{21} - 10^{27}\ cm^{-3}$

- **Characteristic parameters:**
  - Density parameter $r_s = \bar{r}/a_B \sim 1$
  - Degeneracy temperature $\theta = k_B T/E_F \sim 1$
  - $\Theta > 1$: quantum plasma,
    $\Theta < 1$: classical plasma
    Classical coupling parameter $\Gamma = e^2/r_s k_B T \sim 1$

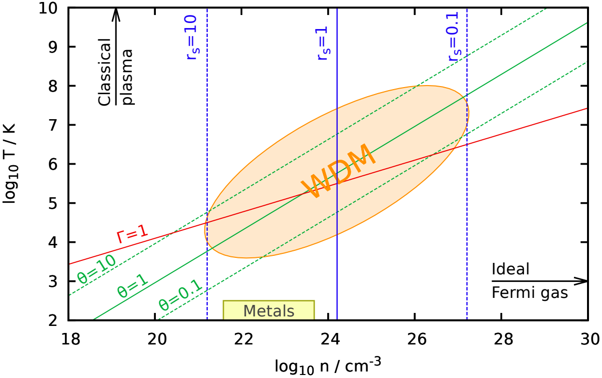

www.theo-physik.uni-kiel.de/bonitz